

Review

Reaction-bonded silicon nitride: its formation and properties

A. J. MOULSON

Department of Ceramics, University of Leeds, Leeds, UK

The theme of the review is the construction of a model embracing the mechanism of formation of reaction-bonded silicon nitride, the development of microstructure and mechanical properties. Possible nitridation reactions are discussed, with emphasis on kinetics and on phase composition and microstructure of the reaction product. The influence of Fe, a common impurity in silicon powders, and of H₂, as an additive to the nitriding atmosphere, is considered in some detail. The optical, electrical and thermal properties are briefly discussed and areas for further research and development studies identified.

1. Scope and purpose of the review

Interest in reaction-bonded silicon nitride (RBSN)* as a high-temperature engineering ceramic was first shown about twenty years ago by Parr of the Admiralty Materials Laboratory, and Popper of the British Ceramic Research Association, both in the United Kingdom. The ceramic attracted interest because of an unusual feature associated with its fabrication and because of its promising thermo-mechanical properties. A modest research and development effort has since been maintained in the United Kingdom, and the material is now commercially available.

In addition to the interest shown in RBSN, there have been parallel efforts to exploit the "hot-pressed" variety of silicon nitride (HPSN), and to evaluate the "sialons". "Nitrogen ceramics" has, in consequence, become an established and potentially important area of ceramics science and technology and, also, a complex one. The present review confines attention to RBSN, and for a wider coverage of nitrogen ceramics reference should be made to two review articles [1, 2] and to the Proceedings of the NATO Advanced Study Institute on Nitrogen Ceramics [3].

In about 1970, the US Government's Advanced Research Projects Agency (ARPA) decided to finance a programme having as a major aim the use

of RBSN in the construction of a small gas-turbine engine for the motor car. This major project currently involves principally the Army Materials and Mechanics Research Center at Watertown, Mass, and the Ford Motor Company. The ARPA project stimulated a world-wide growth of interest with a consequent proliferation of publications concerned with the fabrication science, properties and engineering of RBSN. The extent and nature of this literature confronts the would-be researcher with a difficulty; it has been especially difficult to identify fruitful areas for research with the result that, too frequently, there has been duplication of effort with little advance in understanding. The state of knowledge as it existed a decade ago is well summarized by Parr and May [4], and the early stages of the ARPA programme in the Proceedings of the Hyannis Conference [5].

TABLE I Typical characteristics of "commercial" silicon powder

Major impurity elements	wt%
Fe	0.90
Al	0.20
Ca	0.30
Ti	0.10
Oxygen	1.0
Mean particle size:	15 μm
Specific surface area:	1.5 $\text{m}^2 \text{g}^{-1}$

* The term "reaction-bonded" is preferred to "reaction-sintered" since the word "sinter" usually implies densification by solid-state diffusion processes, which are not significant in the formation of RBSN.

The major aim of the review is to present a model to explain the mechanism of the formation and the mechanical properties of RBSN. It is the hope that the model will allow areas for further study to be more clearly identified than has hitherto been possible, and that improvements in both fabrication route and material properties will follow.

2. Outline of the fabrication route and property requirements of RBSN

RBSN is usually fabricated from "commercial" silicon powder, the typical characteristics of which are given in Table I. First, a silicon powder compact is produced, either as a billet or in the shape of the component being fabricated. It is the common practice to form the billet by isostatic pressing at up to 200 MN m^{-2} ; this is then "pre-sintered" at approximately 1200°C in argon (previously it was the fashion to pre-nitride) after which it can be conventionally machined to the required component shape and dimensions. After shaping, the component is heated, usually in nitrogen at atmospheric pressure and at temperatures in the range 1250 to 1450°C , when reaction-bonding occurs. The silicon powder compact might also be formed directly into the component shape by slip-casting, extrusion, injection-moulding, die-pressing or flame-spraying.

An unusual and attractive feature of the fabrication route is that very little size-change occurs in the compact during nitridation and close tolerances (approximately 0.1%) on the dimensions of a finished component can readily be maintained, thereby avoiding expensive machining after firing.

Typically the ceramic has a porosity of approximately 20 vol%, with 80 vol% of the pores of size less than $0.1 \mu\text{m}$ [6]. The properties of RBSN will be discussed later, and here it is sufficient to say that a combination of ease of fabrication, a low thermal expansion coefficient which reduces the risk of thermally induced failure, useful mechanical strength maintained to high temperatures, and a promising resistance to corrosion, has placed RBSN as a foremost candidate material for high-temperature engineering.

By using ceramics in an engine the consequent increase in operating temperature would improve thermodynamic efficiency. The current maximum working temperature of a gas-turbine with nimonic blades is approximately 1050°C ; it has been estimated that if the target running temperature of

1370°C for the small vehicular gas-turbine is realized, then fuel savings of up to 40% for a given power output are possible. In addition, the engine would be lighter and constructed from cheap and readily available materials.

For these applications, high-temperature mechanical strength and corrosion resistance characteristics of the material must be optimized. In addition, and perhaps more importantly, the Weibull modulus [7], a measure of the reliance to be placed on the strength, needs to be maximized.

The properties of a material are determined in part by its chemical nature and in part by texture. Texture, which is of central interest to the ceramist, can strongly influence the mechanical properties and corrosion-resistance of RBSN [124] and it is for this reason that the emphasis of the present review will be on laying a foundation for a systematic approach to microstructure control.

3. Background basic science of the compound Si_3N_4

It is not the intention to present here a comprehensive review of the extensive literature but to concentrate attention on those facts which are relevant to the preparation and properties of RBSN. Such an overview is essential to the logical development of the review as a whole.

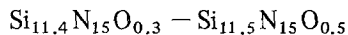
3.1. Crystal structure

Interatomic bonding in crystals is a complex subject discussed, in the case of the nitrogen compounds, by Morgan [8]. Following Pauling [9], the bonding in Si_3N_4 can be estimated to be 70% covalent in character.

Crystalline Si_3N_4 exists in two hexagonal forms designated α and β [10–12], the first complete structure determination having been made by Ruddlesden and Popper [13]. In both forms the basic building unit is the silicon–nitrogen tetrahedron, joined so that each nitrogen is shared by three tetrahedra. For a lucid description of the structure the paper by Thompson and Pratt [14] is recommended.

It was believed that the α - and β -forms were, respectively, low- and high-temperature polymorphs of Si_3N_4 . In 1968, however, Grieveson *et al.* [15] reported that the α - and β -forms were, respectively, "high oxygen potential" and "low oxygen potential" modifications and later [16] they described α - Si_3N_4 as a defect structure with

oxygen replacing nitrogen on some sites and nitrogen vacancies maintaining electrical neutrality. The proposed "oxynitride" was said to have the compositional range:



and thermochemical measurements [17] lent support to this model.

There now seems doubt that $\alpha\text{-Si}_3\text{N}_4$ need contain oxygen [18–21], a view consistent with the structure determinations [20, 22–24] for which it was unnecessary to assume $\alpha\text{-Si}_3\text{N}_4$ to be anything but the stoichiometric nitride.

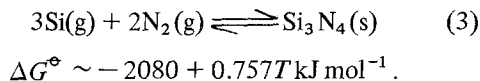
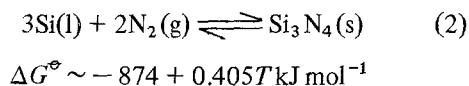
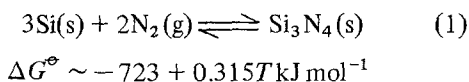
The present consensus of opinion is that α - and $\beta\text{-Si}_3\text{N}_4$ are polymorphs of Si_3N_4 , with $\alpha\text{-Si}_3\text{N}_4$ having the slightly higher free energy at the formation temperature [25, 74]. This does not, of course, preclude the possibility that the α -phase could contain oxygen as an impurity. In fact, there is strong evidence of a direct correlation between the unit cell dimensions of $\alpha\text{-Si}_3\text{N}_4$ and oxygen content [26].

It seems likely that the development of one or other of the two modifications is dictated by the particular growth mechanisms rather than by thermodynamic considerations, and this will be fully discussed later.

3.2. Thermochemical data

3.2.1. Formation and stability of Si_3N_4

Silicon nitride can be formed from its elements according to the following reactions:



The thermodynamic relationships are derived from the basic data generated by Pehlke and Elliott [27], who studied the equilibrium for Reaction 2 between 1400 and 1700°C (m.p. of Si is approximately 1413°C). Reaction 1 is obtained from Reaction 2, using the heat of fusion determined by Olette [28] and Reaction 3 from Reaction 2 using the heat of vaporization determined by Grievson and Alcock [29]. Reactions 1 and 3 apply only to temperatures near to the melting point of silicon.

The X-ray data reported by Pehlke and Elliott indicate that both α - and $\beta\text{-Si}_3\text{N}_4$ were present in their study; for this reason the crystalline form of the silicon nitride is unspecified in Reactions 1 to 3. Both phases would almost certainly have been present in the similar experiments carried out by Hincke and Brantley (1330 to 1530°C) [30], whose results agree well with those of Pehlke and Elliott. The JANAF tables [31], which draw on the results of these studies, incorrectly state that the data refer to the $\alpha\text{-Si}_3\text{N}_4$ phase.

More recently, Blegen [32] studied the equilibrium of $\beta\text{-Si}_3\text{N}_4$ with ferrosilicon alloys between 1400 and 1640°C. Because the activity of silicon in ferrosilicon is lowered relative to that of pure silicon, the equilibrium nitrogen pressures are correspondingly raised to values experimentally more accessible. Blegen's results agreed well with those of Pehlke and Elliott [27] and Hincke and Brantley [30], but not with those of Colquhoun *et al.* [17], who also employed ferrosilicon alloys. Hendry [33] attributed the discrepancy to the different activity values for silicon adopted in the two studies. The scatter in published activity values [34] is an indication of the experimental uncertainty introduced by using this approach. Although Blegen's data are to be preferred at present because of their agreement with those of the independent studies [31], further experimental confirmation would be required before they could be accepted with confidence.

From Fig. 1, showing equilibrium nitrogen pressure as a function of temperature, derived from Reactions 1 and 2, it can be seen that the dissociation temperature, i.e. the temperature at which the equilibrium nitrogen pressure is 1 atm, is about 1900°C. The graph is of practical value in that it defines the minimum nitrogen pressure which must be maintained around the nitride, at any temperature, to prevent dissociation.

Si_3N_4 is unstable with respect to the oxide (SiO_2) and stoichiometric oxynitride ($\text{Si}_2\text{N}_2\text{O}$). For example, at 1400°C the standard free energies ($p_{\text{N}_2} = p_{\text{O}_2} = 1 \text{ atm}$) of formation of Si_3N_4 , SiO_2 and $\text{Si}_2\text{N}_2\text{O}$ are approximately -200 kJ mol^{-1} (Reaction 1), -600 [31] and -460 [32], but nothing definite can be said of the rates of oxidation, the important consideration in the practical application of the ceramic.

The rate of oxidation of RBSN will depend upon microstructure, and the natures of the environment and oxidation product. Davidge

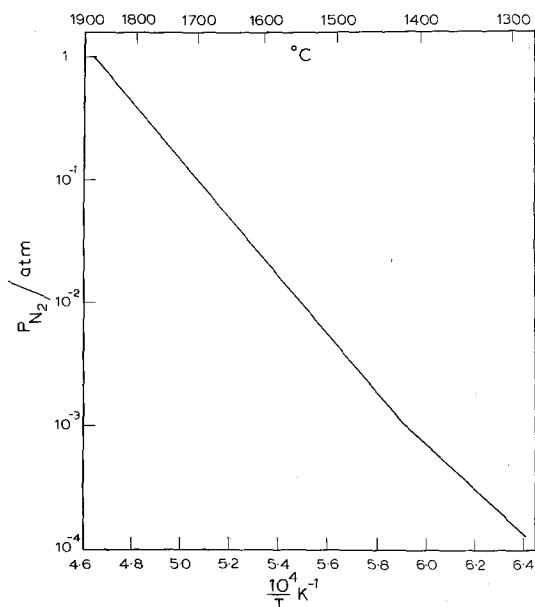


Figure 1 Equilibrium vapour pressure of N_2 over Si_3N_4 .

et al. [35] have discussed oxidation of internal surfaces and development of a protective layer of silica. However, under low oxygen partial pressures “active oxidation” could still occur, the ceramic being continuously degraded by the removal of volatile silicon monoxide; this type of active oxidation, in the case of SiC, has been studied by Hinze and Graham [36]. Mayer and Riley [37, 38] investigated the effects small amounts of sodium salts have on oxidation and point to the important role impurities might have on oxidation

TABLE II Selected data for Si and Si_3N_4

Property	Value	Source
Melting point (Si)	1686 K	[28]
Linear expansion coefficient (Si) (300–1600 K)	$3.92 \times 10^{-6} K^{-1}$	[155]
Density (Si)		
1686 K: solid	$2320 kg m^{-3}$	[155]
1686 K: liquid	$2520 kg m^{-3}$	[156]
Specific volume change on melting (Si)	–86%	from density data
Density (Si_3N_4 crystal phase unspecified)	$3180 kg m^{-3}$	Various sources
Linear expansion coefficient (Si_3N_4) (300–1300 K)	$3.0 \times 10^{-6} K^{-1}$	Various sources
Dissociation temperature (Si_3N_4)	2155 K	Fig. 1

kinetics and to the need for studies on high purity material.

3.2.2. Atom mobility in Si_3N_4

In a gas/solid reaction yielding a solid reaction product, solid-state diffusion in the product may be the rate-determining step. It is for this reason that self-diffusion and lattice defect studies in oxides constitute a major part of corrosion science [39]. An analogous situation exists in the case of the nitridation of silicon in which the mobilities of silicon and nitrogen in silicon nitride, the effect of impurities, and the defect chemistry of silicon nitride would be important aspects.

Self-diffusion data for silicon nitride are sparse, the obstacles to obtaining them being the non-availability of well-defined nitride samples of suitable dimensions and the lack of suitable radioisotopes of Si and N. The difficulties, together with a feasible experimental approach using mass spectrometry, are discussed by Weunsch and Vasilos [40].

Nitrogen self-diffusion in polycrystalline α - and β - Si_3N_4 has been measured by Kijima and Shirasaki [40] using mass spectrometry; the diffusion coefficients they found were:

$$(D_N)_\alpha = 1.2 \times 10^{-16} \exp\left(-\frac{233}{RT}\right) m^2 sec^{-1} \quad (4)$$

$$(D_N)_\beta = 5.8 \times 10^{+2} \exp\left(-\frac{777}{RT}\right) m^2 sec^{-1} \quad (5)$$

in which the activation energy is given in $kJ mol^{-1}$. In view of the similarity of the structures of the α - and β -phases, the very large difference in the pre-exponential terms is surprising and suggests that extrinsic effects were dominating.

Although a refinement of the experimental approach of Atkinson *et al.* [42] might yield the flux of reactants through a pure, coherent nitride film, it would not be possible to relate this to self-diffusion data until information is available regarding the defect chemistry of silicon nitride. As stated by Brook [43] in a recent review, there is virtually no firm knowledge of the defect chemistry of the nitrogen ceramics.

3.2.3. Selected property data

The physical property data in Table II may be helpful to the reader in the development of the subsequent discussions.

4. Development of a model for the reactions occurring during the formation of RBSN from a "commercial" silicon powder

4.1. Requirements of the model

RBSN is formed by heating a silicon powder compact in a nitrogenous atmosphere between 1250 and 1450°C. Typically, the mean particle size of the silicon powder would lie between 10 and 25 μm and the "green" compact density between 1500 and 1600 kg m⁻³. As the reaction proceeds, the compact gains strength with negligible change in dimensions, although the solid volume increases by approximately 22% on conversion to nitride.

RBSN has a porosity of approximately 20%, the nitride being 60 to 90% by weight of the α-phase, and the remainder β-Si₃N₄. There is also, invariably, a residual quantity of finely dispersed, unreacted metallic phase, as shown in Fig. 2, a characteristic micrograph.

An acceptable model for the reactions occurring during the formation of RBSN should be compatible with:

- (i) the dimensions of the compact remaining unchanged on conversion to the nitride;
- (ii) the observed rates of conversion of Si to Si₃N₄;
- (iii) the observation that generally, when the nitriding is carried out at approximately 1350°C in nitrogen at atmospheric pressure, the ratio of α-Si₃N₄ to β-Si₃N₄ (the "α/β ratio") lies in the range 1.5 to 9.0.

The model should also be compatible with experimental data describing the effects on the system of changes in process variables.

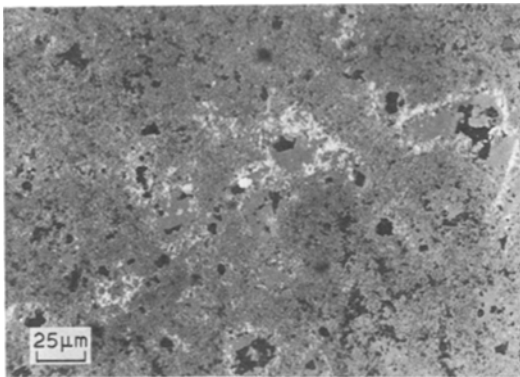


Figure 2 Reflected light optical micrograph of typical commercial RBSN: grey – Si₃N₄; white – unreacted "metallic" phase; black – pores (after Metcalfe [70]).

In the following Sections 4.2 to 4.4, the literature is reviewed and arguments developed preparatory to defining and discussing the model. It might help the reader to refer to the essential features of the model, stated in Section 4.5, before continuing with the present discussion.

4.2. Background studies

In general, attempts to elucidate the process have involved measurement of nitridation kinetics in conjunction with microscopy of the reaction product. Popper and Ruddlesden [44], in one of the first studies, observed approximately parabolic nitridation kinetics but noted inconsistencies which indicated "that some uncontrolled factor was playing a part equally as important as temperature". They also commented that the rates of nitridation measured by many other workers "varied enormously from one laboratory to another" which led them to suspect that "impurities in either the silicon or the nitriding atmosphere have a considerable influence on the nitriding rate". They went on to say that their results demonstrated the need for kinetics studies with emphasis placed on careful control of chemical composition of the silicon and nitriding atmosphere. In retrospect this paper would have been a firm foundation on which subsequent research should have been based.

Thompson and Pratt [14] proposed a mechanism for the development of the microstructure and phase composition of RBSN as follows. During nitriding below the melting point of silicon, a thin film of nitride forms on the silicon: because of the compressive strain in the film, microcracks are produced, exposing the silicon which allows the reaction to continue. The nitride film breaks away from the silicon and continuation of this process gradually fills the pore space with "flakes" – observed as the "diffuse" regions of the microstructure. Above the melting point of silicon they observed growth morphologies of the type shown in Fig. 9.

In a later study, Dagleish and Pratt [45] gave the following summary of the developing microstructure:

"X-ray studies have shown that during the initial stages of nitridation α-Si₃N₄ is formed, while electron microscope studies have shown that the fine-grained matrix is predominantly α-Si₃N₄ and that the large grains are mainly

β - Si_3N_4 . The early stages of nitridation, therefore, lead mainly to the formation of the background mat.

At temperatures below the melting point of silicon, the pores of the silicon compact become filled with needles. Continued reaction increases the number and thickness of the needles which grow together and generate the fine-grained matrix. At the same time small areas of silicon are converted to granular Si_3N_4 .

When the temperature of nitridation is increased above the melting point of silicon, there is increased formation of β -silicon nitride as crystallites grow into the molten silicon held within the matrix. Prolonged reaction above the melting point of silicon results in the conversion of residual silicon to granular silicon nitride and densification of the background mat, until the formation of the two-phase structure, discrete β - Si_3N_4 grains surrounded by a dense mat of α - Si_3N_4 , is complete."

As far as understanding the mechanism of the reaction was concerned, however, little progress had been made. Messier and Wong [46], in attempting to separate out the effects of the many variables, recognized that iron impurity, through the development of molten FeSi_x , could influence the course of the reaction. Furthermore, they observed that, under certain conditions, an oxide film on the silicon could also affect the reaction.

The prevailing view regarding the nature of the reaction product was that the formation of an α - Si_3N_4 whisker mat predominates [47, 45] and that this growth probably develops as a result of the reaction between volatile SiO and N_2 . This particular reaction had gained favour because it was the basis of the production of high strength α - Si_3N_4 whiskers for composite reinforcement material [48–50].

TABLE III The effect of O_2 and H_2O additions to N_2 on reaction products.

O_2 in N_2 (ppm by volume)	H_2O in N_2 (ppm by volume)	α/β ratio at 50% Si conversion	Reaction products
0	40	0.6	Si_3N_4 + trace Si
50	40	0.6	Si_3N_4 + trace Si
1 000	100	0.6	Si_3N_4 + trace Si
5 000	200	0.6	Si_3N_4 + trace Si
15 000	200	0.2	Si_3N_4 + trace $\text{Si}_2\text{N}_2\text{O}$
50	70	0.6	Si_3N_4 + trace Si
50	1 000	1.2	Si_3N_4 + trace Si
50	5 000	1.6	Si_3N_4 + trace Si
50	15 000	2.8	Si_3N_4 + trace SiO_2

Around 1972, therefore, although there was no firm knowledge of the nitridation reaction mechanism, it was generally believed that:

(i) the formation of α - Si_3N_4 was favoured at reaction temperatures below and β - Si_3N_4 above the melting point of silicon;

(ii) the steady development of an α - Si_3N_4 whisker mat was responsible for the increase in mechanical strength during reaction-bonding; and

(iii) various impurities (Fe , O_2) affected the course of the reaction.

4.3. Post 1970 studies at Leeds

The reason for the poor understanding of the reaction mechanism was that little attempt had been made to bring the many variables, particularly the chemical impurities associated with the Si powder, under control. With Science Research Council support, work was started at Leeds in 1970 to elucidate the reaction mechanism, a major feature of the research to be control over chemical variables. This was a first step towards achieving an understanding of the bonding mechanism, the ultimate goal being to effect control over microstructure. The studies are reviewed below.

4.3.1. Preliminary experiments

It had already been shown that surprisingly large quantities of oxygen and water-vapour could be added to the nitriding atmosphere without inhibiting nitridation of commercial silicon powder [51]. The data, summarized in Fig. 3 and Table III, are discussed later.

It had also been confirmed that cation impurities (1 wt % Mn, Fe, Co or Ni) added to a high-purity silicon powder had a very marked accelerating effect on nitridation [52, 53]. In contrast, silicon powder, deliberately partially oxidized so that a $1\ \mu\text{m}$ thick oxide layer covered the particles, could not be nitrided, although reactivity was

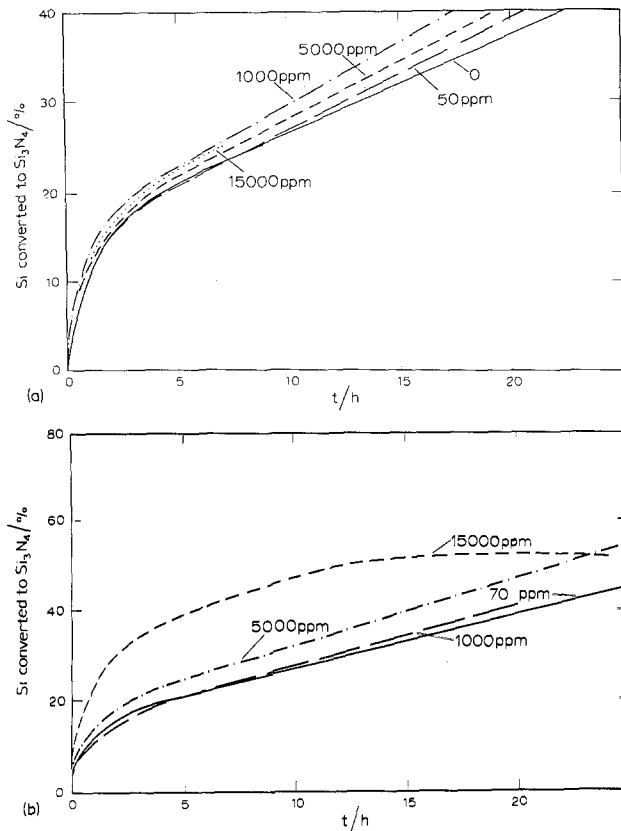


Figure 3 The effect of (a) O₂ additions and (b) H₂O additions, to N₂ on the nitriding of "commercial" silicon powder (~98 wt% Si) at 1370° C.

completely restored by the subsequent addition of 10 wt % Fe₂O₃ [51].

It was recognized that nitridation of a compact must involve two steps, namely: (1) movement of nitrogen into the continuously changing pore system of the compact, and (2) chemical reaction between silicon and nitrogen, the slower being the rate-determining step. Also, the exothermic reaction (Reactions 1 to 3) would produce temperature gradients in a compact, and quantitative knowledge of these would be needed if meaningful data relating to the temperature dependence of the reaction were to be obtained.

To summarize, it was acknowledged that the effect of the following factors would need to be examined:

(a) gas-permeability of the nitriding compact, and the conditions under which it would constitute a reaction rate-determining parameter;

(b) temperature gradients within the compact; and

(c) impurities in the nitriding gas, principally O₂ and H₂O, and those associated with the silicon, particularly Fe and O₂. (The oxygen associated with the silicon, particles is in the form of a silica

coating, typically 3 nm thick [53], and usually referred to as the "native" silica film.)

Subsidiary studies [54, 55] had established the conditions under which (a) and (b) would be insignificant. The variables detailed under (c) could be controlled by using high purity, laboratory-prepared silicon powder and by measuring the kinetics in a specially designed thermogravimetric balance. The main studies [42, 56, 57] are outlined in the next section.

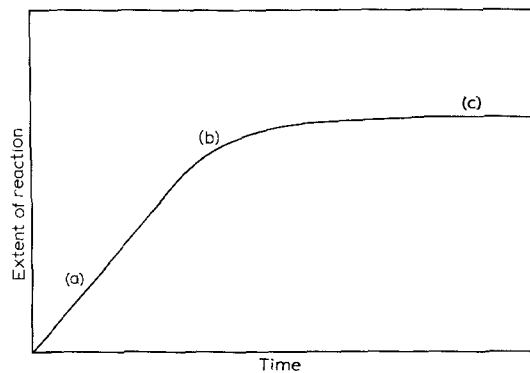
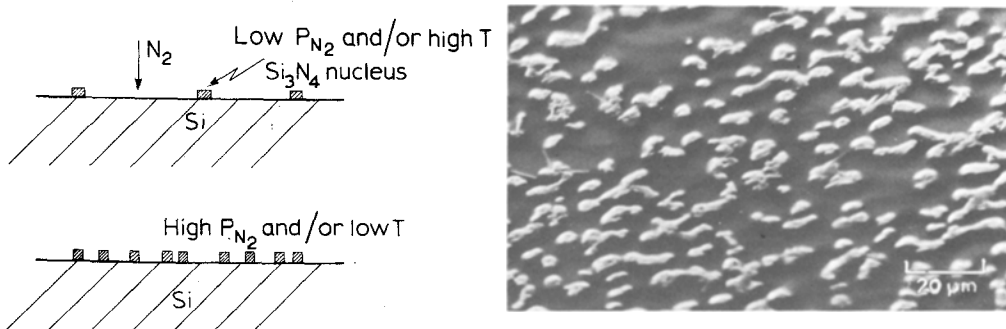
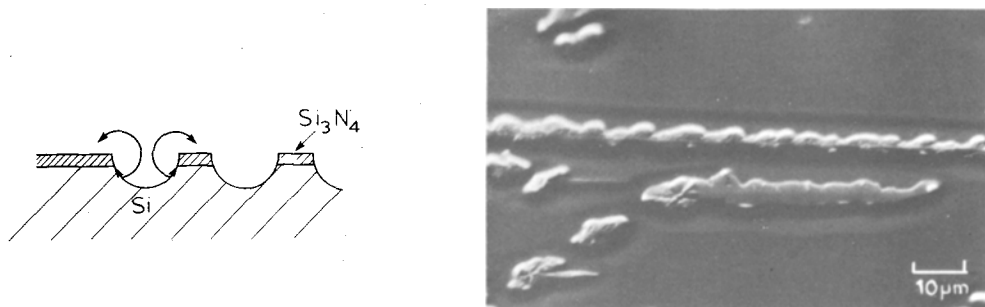


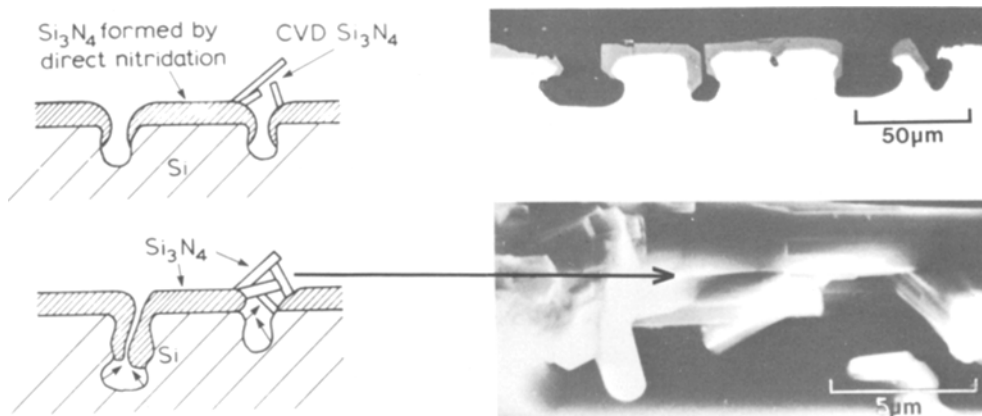
Figure 4 Schematic of reaction kinetics showing the three regimes: (a) linear kinetics, (b) decreasing reaction rate, (c) effectively "zero" reaction rate, even though compact is only partially nitrided.



(i) Formation of Si₃N₄ nuclei on Si surface: areal density of nuclei increases as p_{N_2} increases and T decreases.



(ii) Nuclei grow laterally and vertically: Si supplied to growth sites by combination of surface diffusion and evaporation. Rate of arrival of nitrogen to growth site determines reaction rate for $p_{N_2} \leq 1$ atm, at least.



(iii) As free Si surface area decreases, surface diffusion distances increase and so direct nitridation slows. Reaction of Si in the vapour state to form a complex which subsequently condenses, continues. 'Zero' reaction rate when reactants effectively separated.

Figure 5 Stages through the course of the reaction between pure Si and N₂.

4.3.2. Studies with high-purity silicon

Silicon powder was prepared from semiconductor-grade ingot, and a compact size chosen so that gas-permeation and exotherm effects were negligible. The impurities were known to be at the ppm level and the equipment afforded the facility for removing the native silica film. The nitridation kinetics, measured as a function of temperature (1250 to 1370°C) and nitrogen pressure (20 to 760 Torr), could be described in terms of three regimes, as shown in Fig. 4.

By correlating the developing microstructure with kinetics, the reaction-model shown schematically in Fig. 5 was proposed.

The first stage involves the formation of Si₃N₄ nuclei on the Si surface, followed by their growth, thought to be by the reaction between chemisorbed nitrogen and silicon, the latter arriving at the reaction site by a combination of surface diffusion and an evaporation/condensation process. During this stage the kinetics are linear with time. As the nitrided layer extends over the

surface, supply of Si to reaction sites decreases and, in consequence, so too do the kinetics. Finally, as the film effectively separates the reactants, the rate falls to nearly zero. The model qualitatively explained the dependence of the kinetics on changes in temperature and nitrogen pressure.

The phase composition of the growth was studied by Longland and Moulson [57] whose data are summarized in Fig. 6. The curves describe the development of the α - and β - Si_3N_4 as nitridation proceeds. Under the special, low nitrogen pressures, the supply of nitrogen to the reaction sites is rate-determining to approximately 70% conversion, and the α - and β - Si_3N_4 forming reactions are, therefore, competing for nitrogen. Consideration of the curves and of Fig. 5 leave little doubt that nitridation on the Si surface leads to the formation of β - Si_3N_4 , as previously suggested by Horsley [58] and Blegen [32], while the vapour-phase reaction leads to α - Si_3N_4 . It is apparent that as the β -forming reaction slows, because surface diffusion distances for Si increase, the α -forming vapour-phase reaction continues.

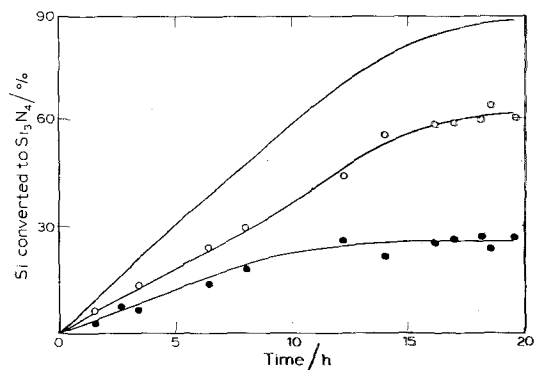


Figure 6 Growth kinetics of α - Si_3N_4 and β - Si_3N_4 (99.999% Si, $< 45 \mu\text{m}$; 1370°C and 50 Torr N_2): — total; \circ α - Si_3N_4 ; \bullet β - Si_3N_4 .

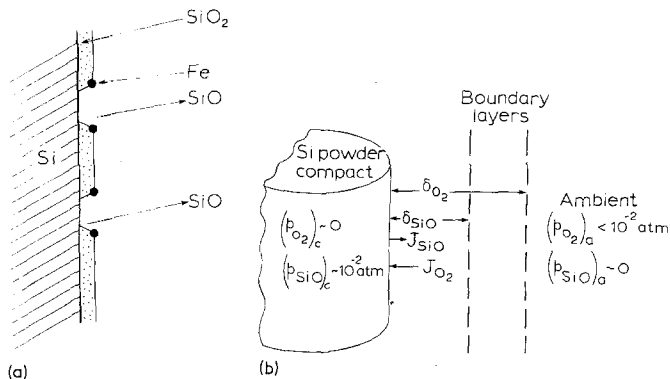


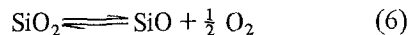
Figure 7 (a) Fe-induced evaporation of surface SiO_2 as SiO . Fe disrupts (devitrifies) SiO_2 film allowing Equilibrium 8 to be established; film evaporates as SiO . (b) Exchange of SiO and O_2 between compact and ambient.

* Throughout the text p_{SiO} etc. refer to partial pressures of the particular gas or vapour, measured in atmospheres.

4.3.3. The effect of additions of Fe, a major impurity in commercial silicon, on the nitriding of high purity silicon

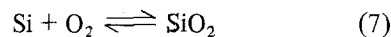
Boyer *et al.* [59], from an analysis of Atkinson's [42] data, and from additional measurements of the rate of oxidation of iron-contaminated silicon powder, proposed a model to explain the effect of iron impurity on nitridation. They confirmed that Fe first induced the volatilization of the native oxide layer on each particle and led to the growth of extra nitride in proportion to the amount of Fe.

Evidence was already strong [53, 60] that Fe promoted volatilization of the SiO_2 within the first hour of the reaction, the following general argument being advanced to explain the process. Dissociation of the SiO_2 would occur according to:



for which p_{SiO} depends upon p_{O_2} *. However, continuous evaporation can only take place if the removal of oxygen as SiO from the powder compact exceeds the flux of oxygen into it. This is, of course, the essence of Wagner's theory of "active oxidation" [61] which is considered in more detail later in this section.

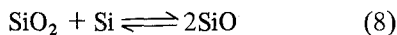
Because of the tendency of the Si underlying the SiO_2 coating on each particle to oxidize, the p_{O_2} within the powder compact might fall. Conditions would, therefore, move towards those expressed by the following equilibrium:



for which p_{O_2} is $\sim 10^{-19}$ atm (at 1350°C). If this p_{O_2} were approached within the compact, then,

by Reaction 6 the p_{SiO} would approach 10^{-2} atm (see Section 4.4.1.2). If the SiO is not involved in any reaction then there will be a nett loss of oxygen from the compact, provided p_{O_2} in the surroundings is less than approximately 10^{-2} atm.

Atkinson and Moulson [60] suggested that the Fe might assist this process by facilitating oxidation of the Si, through enhanced oxygen ion mobility in the SiO_2 . Boyer *et al.* [59] developed this theme suggesting that Fe devitrified the amorphous silica film [62], leading to its disruption, the resulting direct exposure of the underlying Si then allowing the equilibrium:



for which p_{SiO} is $\sim 10^{-2}$, to be rapidly approached. The mechanism is shown schematically in Fig. 7a.

The removal of SiO_2 as SiO from the compact is now considered in more detail. Fig. 7b shows the situation with SiO diffusing away from, and oxygen diffusing towards a silicon powder compact. Within the compact the p_{SiO} is assumed to be at the equilibrium value for Reaction 8, and p_{O_2} at the equilibrium value for Reaction 7, which is negligibly small. Outside the respective boundary layers of width δ , p_{O_2} would be fixed by the purity of the nitriding gas (namely $\ll 10^{-2}$ atm) and the p_{SiO} would be negligible.

A state of dynamic equilibrium exists when J_{SiO} from the surface equals J_{O} towards the surface, where

$$J_{\text{SiO}} = -D_{\text{SiO}} \frac{(p_{\text{SiO}})_c}{RT} \frac{1}{\delta_{\text{SiO}}} \text{ mol m}^{-2} \text{ sec}^{-1} \quad (9)$$

$$J_{\text{O}} = -2D_{\text{O}} \frac{(p_{\text{O}_2})_a}{RT} \frac{1}{\delta_{\text{O}_2}} \text{ mol m}^{-2} \text{ sec}^{-1} \quad (10)$$

the subscripts c and a referring to the "compact" and "ambient", respectively, the D is the appropriate diffusion coefficient and the factor 2 arises because molecules of oxygen convey two atoms each.

For nett removal of SiO, $J_{\text{SiO}} > J_{\text{O}}$, i.e.

$$D_{\text{SiO}} \frac{(p_{\text{SiO}})_c}{RT} \cdot \frac{1}{\delta_{\text{SiO}}} > 2D_{\text{O}} \frac{(p_{\text{O}_2})_a}{RT} \cdot \frac{1}{\delta_{\text{O}_2}},$$

and

$$(p_{\text{O}_2})_a < \frac{1}{2} \frac{(p_{\text{SiO}})_c}{D_{\text{O}}} \frac{D_{\text{SiO}}}{D_{\text{O}}} \cdot \frac{\delta_{\text{O}_2}}{\delta_{\text{SiO}}}$$

which, after Wagner, can be written approximately as:

$$(p_{\text{O}_2})_a < \frac{1}{2} (p_{\text{SiO}})_c. \quad (11)$$

Under these circumstances, first the native silica layer and then the silicon will be removed as SiO.

Boyer and Moulson [63] extended the range of Fe-doping of high purity silicon powder to 5000 ppm (i.e. 0.5 wt %) and established that both phase composition and extent of the extra nitride growth could be correlated with Fe content. Fig. 8 shows that, for a fixed reaction time of 10 h, there was extra conversion of Si to $\beta\text{-Si}_3\text{N}_4$

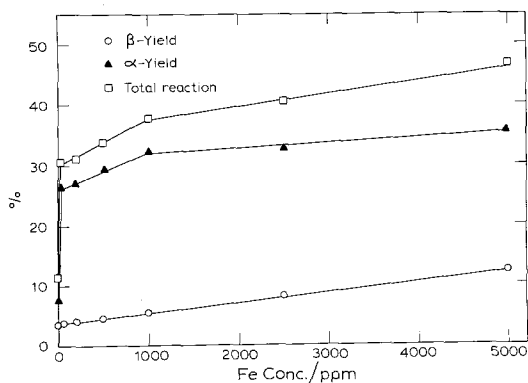


Figure 8 Dependence of α - and $\beta\text{-Si}_3\text{N}_4$ -yields on Fe addition: high purity Si + Fe; 1350° C for 10 h; 760 Torr N_2 . (After Boyer and Moulson [63]). Note: some authors use the term "alpha-yield" and "beta-yield". The "alpha-yield" is defined as the product of the percentage of Si converted to Si_3N_4 and the fraction of the nitride of the α -phase; this represents the percentage of Si converted to $\alpha\text{-Si}_3\text{N}_4$. The "beta-yield" is defined similarly.

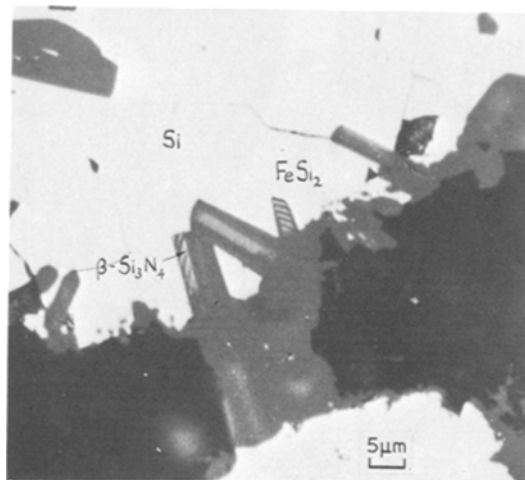


Figure 9 Optical micrograph showing $\beta\text{-Si}_3\text{N}_4$ growing into FeSi_2 phase, molten at reaction temperature (after Boyer and Moulson [63]).

proportional to the amount of Fe added, and microstructural evidence (Fig. 9) leaves no doubt that this β -phase was growing into FeSi_2 , known from the Fe/Si phase diagram [34] to be liquid at the reaction temperature. Fig. 8 also shows that while the extent of the total reaction varied linearly with the Fe added in amounts up to approximately 1000 ppm, relatively smaller conversions were obtained for larger additions because of a decrease in the rate of the α -forming reaction.

To summarize, it is believed that Fe additions can:

(1) catalyse the removal, as SiO , of the native oxide film covering the silicon particles;

(2) promote growth of $\beta\text{-Si}_3\text{N}_4$ in FeSi_2 , liquid at the reaction temperature, the Fe-induced growth in a fixed time at constant temperature (10h and 1350°C in the present case) being proportional to the amount of Fe added to the powder;

(3) promote growth of $\alpha\text{-Si}_3\text{N}_4$, although a proportionality similar to that referred to in (2) does not hold.

The various processes are shown schematically in Fig. 10.

4.4. Consideration of possible nitridation reactions

4.4.1. Compatibility with observed kinetics

In this section, throughout which orders of magnitude only of the parameters are quoted, consideration is given to various nitridation reactions possible in a commercial silicon powder compact heated at 1350°C in nitrogen, arbitrarily assumed to contain 10 ppm of O_2 and of H_2O .* The thermodynamic data are drawn from the JANAF tables [31].

It will be recalled that an acceptable model should be compatible with observed nitridation kinetics. From the many published data (e.g. [14, 53] and Fig. 12), and assuming that the silicon powders would have a specific surface area of approximately $1\text{ m}^2\text{ g}^{-1}$, it is estimated that the highest reaction rates observed are $10^{-7}\text{ kg m}^{-2}\text{ sec}^{-1}$. That is, in the initial stages of nitridation, approximately 10^{-7} kg silicon is converted to nitride per second per unit total surface area of compact.

4.4.1.1. Nitridation of volatilized Si. The vapour pressure of Si at 1350°C is 10^{-7} atm and this

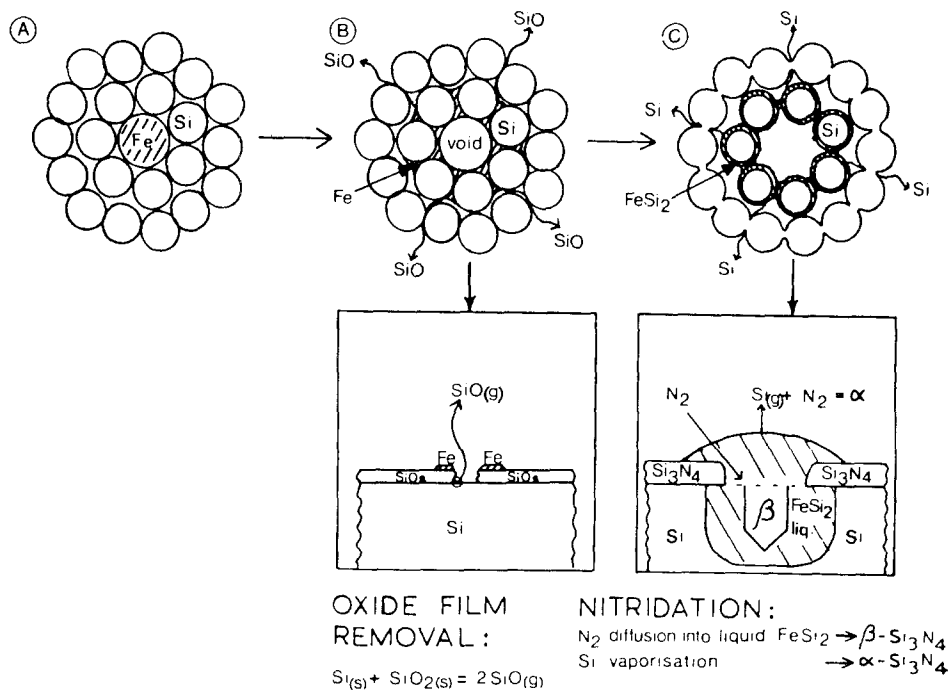


Figure 10 Schematic of role of Fe in nitridation reaction (after Boyer and Moulson [63]).

* The arguments retain their validity for higher levels, e.g. 1000 ppm (10^{-3} atm).

implies a rate of evaporation of silicon of $10^{-6} \text{ kg m}^{-2} \text{ sec}^{-1}$ [64]. The supply of Si vapour, then, and its subsequent reaction with the nitrogen ($p_{\text{N}_2} = 1 \text{ atm}$) according to Reaction 3, is more than adequate to sustain the observed reaction rates.

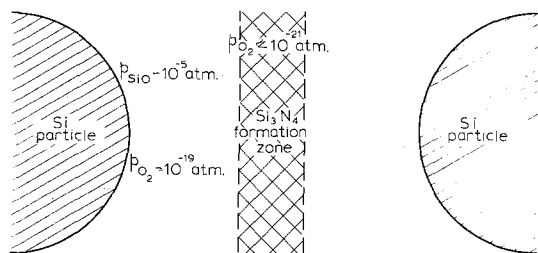
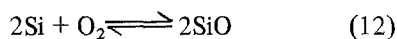


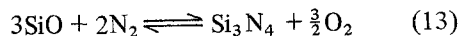
Figure 11 Schematic of conditions for nitridation of SiO in the interior of a Si powder compact.

4.4.1.2. Nitridation of SiO originating from oxygen in nitriding gas. ($p_{\text{N}_2} = 1 \text{ atm}$; $p_{\text{O}_2} \sim 10^{-5} \text{ atm}$) The argument in this case is complex, and it will be helpful to refer to Fig. 11, which depicts the local situation within a compact. Consider first the equilibrium:



for which $\Delta G^\circ = -477 \text{ kJ mol}^{-1} = -RT/\ln p_{\text{SiO}}^2/p_{\text{O}_2}$. It follows that $p_{\text{SiO}}^2/p_{\text{O}_2} \sim 10^{15}$ and, if $p_{\text{O}_2} \sim 10^{-19}$, then $p_{\text{SiO}} \sim 10^{-2}$. However, the actual p_{SiO} would be limited, by the availability of O_2 , to approximately 10^{-5} .

The nitridation of SiO is assumed to be according to the following reaction:



for which $\Delta G^\circ = 502 \text{ kJ mol}^{-1}$ and the equilibrium constant,

$$k = p_{\text{O}_2}^{3/2}/p_{\text{SiO}}^3 p_{\text{N}_2}^2 = 7 \times 10^{-17}.$$

Under the assumptions that $p_{\text{SiO}} = 10^{-5} \text{ atm}$ and $p_{\text{N}_2} = 1 \text{ atm}$, then p_{O_2} must be maintained at $\sim 10^{-21} \text{ atm}$.

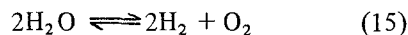
The rate of nitridation of the SiO will be determined by the O_2 flux from the reaction zone and, because the thermodynamics requires that in the zone the p_{O_2} is negligibly small ($< 10^{-21} \text{ atm}$), the flux of oxygen will be correspondingly negligible, or even negative. The observed reaction rates could not, therefore, be sustained by Reaction 13.

4.4.1.3. Nitridation of SiO originating from H_2O in nitriding gas. ($p_{\text{N}_2} = 1 \text{ atm}$; $p_{\text{H}_2\text{O}} = 10^{-5} \text{ atm}$) The situation outlined in Section 4.4.1.2 is modified because H_2 will be generated by the reaction:



for which $\Delta G^\circ = -84 \text{ kJ mol}^{-1}$. Since the equilibrium is well in favour of the products, $p_{\text{SiO}} \sim p_{\text{H}_2} \sim 10^{-5}$.

The equilibrium,



for which $\Delta G^\circ = 314 \text{ kJ mol}^{-1}$, and the equilibrium constant, $k = p_{\text{H}_2}^2 p_{\text{O}_2}/p_{\text{H}_2\text{O}}^2 \sim 10^{-10}$, is also involved. It follows that $p_{\text{O}_2} = 10^{-10} p_{\text{H}_2\text{O}}^2/p_{\text{H}_2}^2$ and $p_{\text{O}_2} \sim p_{\text{H}_2\text{O}}^2$ since $p_{\text{H}_2} \sim 10^{-5}$. Therefore, for the nitridation of SiO according to Reaction 13, which requires p_{O_2} to be $\sim 10^{-21} \text{ atm}$, $p_{\text{H}_2\text{O}}$ must be $\sim 10^{-10} \text{ atm}$.

This necessary low partial pressure of H_2O within a compact will, in general, be difficult to achieve, although it is possible that local accumulations of hydrogen could produce favourable thermodynamic conditions for nitridation.

4.4.1.4. Nitridation of SiO originating from O_2 and H_2O in the nitriding gas, with H_2 added. ($p_{\text{N}_2} = 1 \text{ atm}$; $p_{\text{H}_2\text{O}} = 10^{-5}$; $p_{\text{H}_2} = 10^{-x} \text{ atm}$) Considering again Reaction 15 for the water equilibrium, namely $p_{\text{O}_2} = 10^{-10} p_{\text{H}_2\text{O}}^2/p_{\text{H}_2}^2$ with p_{H_2} put at 10^{-x} atm . It follows that $p_{\text{O}_2} = 10^{2x-10} p_{\text{H}_2\text{O}}^2$. We now consider the pressures of H_2 necessary to maintain, in the reaction zone, a $p_{\text{O}_2} \sim 10^{-21} \text{ atm}$, in equilibrium with $p_{\text{H}_2\text{O}}$ values such that the flux of H_2O away is able to sustain observed nitridation rates; that is, $p_{\text{H}_2\text{O}}$ values of order 10^{-7} atm at least.

For $x = 3$ (i.e. 0.1 vol % H_2 added)

$$p_{\text{O}_2} = 10^{-4} p_{\text{H}_2\text{O}}^2$$

and $p_{\text{H}_2\text{O}}$ must be $\leq 10^{-8} \text{ atm}$.

For $x = 2$ (i.e. 1 vol % H_2 added)

$$p_{\text{O}_2} = 10^{-6} p_{\text{H}_2\text{O}}^2$$

and $p_{\text{H}_2\text{O}}$ must be $\leq 10^{-7} \text{ atm}$.

For $x = 1$ (i.e. 10 vol % H_2 added)

$$p_{\text{O}_2} = 10^{-8} p_{\text{H}_2\text{O}}^2$$

and $p_{\text{H}_2\text{O}}$ must be $\leq 10^{-6} \text{ atm}$.

The calculations offer a possible explanation of why a small addition of hydrogen to the nitriding

gas has such a pronounced effect on nitridation rate (Fig. 12).

4.4.1.5. Nitridation of solid silicon by gaseous nitrogen. This mechanism, outlined in Section 4.3.2, leads to a coherent layer of silicon nitride. The formation of such a layer is rapid when $p_{N_2} = 1$ atm, but can be delayed, permitting continued nitridation of the silicon, if p_{N_2} is reduced (e.g. 50 to 200 Torr).

4.4.1.6. Nitridation of Fe-contaminated silicon. Commercial silicon powders contain typically 0.9 wt% Fe, of which approximately two-thirds is metallic introduced in the grinding process, which is usually done in steel ball-mills [65, 66]. There is, therefore, no doubt that molten $FeSi_x$ will be present at nitriding temperatures above 1207° C [34]. Indeed, because of aluminium, another major impurity, liquid would be expected to form at temperatures even lower than 1207° C and, in fact, this has been confirmed [65]. The evidence provided by kinetics data [42] and microstructural observations [63] shows conclusively that molten $FeSi_2$ is associated with accelerated growth of nitride. This fast growth of nitride in the melt occurs by a VLS mechanism as proposed by Kaiser and Thurmond [67].

A further factor affecting kinetics might be movement of the melt in the powder compact. From contact angle data [68, 69] and other observations [47], spreading of the melt from the Fe source out into the compact microstructure, as shown schematically in Fig. 10, would be expected. The resulting increase in reactive surface, remaining free of reaction-inhibiting nitride growth [67], could explain the observed accelerated reaction. Such a melt would provide a route for silicon to move from the solid to the vapour state, where it can react with the nitrogen.

4.4.1.7. Nitridation of SiO originating from the surface SiO_2 . The Fe-activated removal of the SiO_2 film as SiO has been discussed in Section 4.3.3, and although relatively high (10^{-2} atm) pressures of SiO can be quickly generated, the same problems as outlined in Section 4.4.1.2 above exist as far as its nitridation is concerned. The higher p_{SiO} does increase the critical p_{O_2} to $\sim 10^{-15}$ atm and this can be in equilibrium with $p_{H_2O} \sim 10^{-7}$ and $p_{H_2} \sim 10^{-5}$. In the initial

stages of the reaction, therefore, sufficient hydrogen might be generated by Reaction 14 to allow nitridation of the SiO.

4.4.2. Phase composition of reaction product

4.4.2.1. Reactions forming $\beta-Si_3N_4$. The established correlation between the amount of $\beta-Si_3N_4$ developed and Fe added [63] is consistent with the typical α/β ratios found in commercial RBSN [6, 47, 70]. This is not to imply that α/β ratio is a function of Fe content only; it does, in fact, depend markedly on the particular nitriding temperature schedule and can be varied between the two extreme values. It is accepted that high nitriding temperatures favour the growth of $\beta-Si_3N_4$ [6, 47, 71, 72] and the evidence is that the presence of liquid at the reaction temperature, rather than the presence of Fe, is significant.

Liquid favours growth of $\beta-Si_3N_4$ probably for the same reason as it promotes conversion of α - to $\beta-Si_3N_4$. The model by Bowen *et al.* [73] for this phase-conversion during the hot-pressing of Si_3N_4 , and the study by Messier *et al.* [74], show that conversion requires liquid. The latter workers were unable to detect conversion in powdered high purity CVD $\alpha-Si_3N_4$ heated at 1600° C for 6 h; the addition of MgO, however, promoted some conversion, the MgO-surface SiO_2 reaction producing the necessary liquid at 1600° C.

There is also evidence that the reaction between N_2 and solid silicon leads to $\beta-Si_3N_4$, as discussed in Section 4.3.2. *Therefore, the hypothesis is proposed that, during the formation of RBSN, the major growth of $\beta-Si_3N_4$ occurs in the liquid phase and, to a minor extent, as the result of the reaction between solid silicon and nitrogen.*

The caution to be exercised in the interpretation of experimental data relating to the growth of the α - and $\beta-Si_3N_4$ must be stressed. For example, since it is established that $\alpha-Si_3N_4$ converts to $\beta-Si_3N_4$ in the presence of a liquid and at a significant rate at temperatures [75] commonly encountered in studies [72, 76] in which the growth of one or other phase is of interest, there is the possibility of conversion subsequent to growth. Again, Guthrie and Riley [77] found that the amount of $\beta-Si_3N_4$ grown on similar single crystal Si slices correlated with contamination expected from the alumina envelopes to the

reaction zone. That such contamination is of a nature likely to provide the liquid to account for the observation is beyond dispute [78–80].

4.4.2.2. Reactions forming α -Si₃N₄. It is well documented that CVD Si₃N₄ grows in the α -form [26]* although the morphology is strongly dependent upon the experimental conditions [21]. In the formation of RBSN, the evidence, discussed fully in Section 4.5, points strongly to the formation of α -Si₃N₄ by vapour phase reactions. *Therefore, the hypothesis is proposed that, during the formation of RBSN, the growth of α -Si₃N₄ occurs by vapour-phase reactions.*

Since it is known that α -Si₃N₄ can be precipitated from steels, as pointed out by Grievenson in the discussion following Blegen's [32] paper, the stated hypothesis applies only to RBSN. Whether α - or β -Si₃N₄ grows in any particular situation seems to depend upon the freedom the species have to order themselves into the energetically favoured β -Si₃N₄ modification at the growth sites. When growth occurs in liquid, or on a Si surface where the independent mobility of reactants is high, then such freedom does exist. On the other hand, freedom is clearly restricted in the special situation obtaining when precipitation occurs in a host solid, as in the case of growth in steel.

The reason α -Si₃N₄ forms invariably from vapour-phase reactions may be related to the difficulty S–N complexes, formed in the vapour state, have in adopting the β -Si₃N₄ structure. This is a view closely related to that of Henderson and Taylor [25].

4.4.2.3. Morphology of reaction product. There are many examples in the literature showing the typical morphology of β -Si₃N₄ grown in a liquid [14, 58, 72, 81], the characteristic feature being well-formed crystals of the type shown in Fig. 9. There is evidence (Section 4.3.2) that β -Si₃N₄ can also develop as a dense, coherent layer, the product of the nitridation of solid Si by N₂.

It is reported that β -Si₃N₄ can grow with a whisker-like morphology [82] but in this instance the experimental conditions strongly suggest transformation subsequent to growth. The claim

that β -Si₃N₄ may develop having a "ladder-like" morphology [83, 84] is mistaken; the barred images frequently seen in optical micrographs (cf. Fig. 9) of silicon nitride, and other transparent ceramics, are, of course, optical interference effects [85].

The morphology of α -Si₃N₄ is very dependent upon the growth conditions [21]. This is not unique to Si₃N₄ but is also a feature of the growth from the vapour of, for example, ice [86] and SiC [87]. In the case of α -Si₃N₄, the whisker morphology can develop by a vapour-phase reaction involving the SiO molecule, but there is no evidence that whiskers cannot be produced by other reactions.

It has been suggested [88] that α -Si₃N₄ needles can grow by the VLS mechanism. The fact that this would involve α -Si₃N₄ forming in a liquid constitutes an exception to the rule worthy of closer study.

4.5. A model for the reactions occurring during the formation of RBSN

In Section 4.1 the requirements of a model for the reactions occurring during the formation of RBSN under normal nitriding conditions were defined. Such a model is now stated and the evidence for it discussed.

(1) The dominant process is volatilization of Si and the vapour-phase reaction with N₂; a CVD process leading to the formation of α -Si₃N₄.

(2) Solution of nitrogen in liquid silicon alloys occurs with formation of β -Si₃N₄; essentially a VLS reaction process.

A minor process leading to the growth of β -Si₃N₄ involves nucleation of Si₃N₄ on solid silicon and subsequent growth, following surface diffusion of Si to the reaction site.

A characteristic feature of the nitridation reaction is that the overall dimensions of the "green" compact do not sensibly change, despite a 22% increase in volume on conversion of Si to Si₃N₄. The reactions stated above are compatible with this since they permit the growth of nitride within, and unrestrained by, the compact.

The rate of vaporization of Si and its subsequent nitridation fits the observed kinetics. The vapour-phase nitridation of SiO, the long favoured

* An apparent exception is wrongly referenced; the correct reference is Nickl and Von Braunmüle, [157]. These workers observed Si, α -Si₃N₄ and, possibly, β -Si₃N₄ in CVD material. Nitridation of the Si, subsequent to its deposition, could have led to the formation of β -Si₃N₄. The fine dispersions of Si in RBSN (Fig. 2) might be vapour-deposited in a similar way.

route and invoked again recently [89, 90], is inadmissible on the grounds of the kinetics argument outlined in Section 4.4.1.2. Apart from incompatibility with the kinetics, the observed growth morphologies are not consistent with a predominantly SiO/N₂ reaction. "Whiskers" would be expected to be the product of such a reaction, and yet none were seen in a sample, pre-treated to remove surface SiO₂ but otherwise nitrated normally, to yield 90% α -Si₃N₄ [91]. There is additional similar evidence more appropriately discussed in Section 6.

The model is also consistent with observed α/β ratios which, for commercial RBSN, usually fall in the range 1.5 to 9.0. The thesis of the following discussion is that the dominant vapour-phase reactions produce α -Si₃N₄, with β -Si₃N₄ being formed by VLS and, to a minor extent, by solid Si/N₂ reactions. The nitridation of solid Si by N₂ is an essential element of the model developed by Atkinson *et al.* [42] which explains, for the nitridation of pure silicon, the response of kinetics and microstructure to changes in temperature and nitrogen pressure. It is known (Fig. 12) that the kinetics for a commercial powder respond to changes in p_{N_2} in a generally similar way, indicating that a similar nucleation and growth mechanism operates. According to the Atkinson model, under normal conditions (i.e. $p_{N_2} = 1$ atm), the amount of nitride formed in this way would be small. The proportion of β -Si₃N₄ will, therefore, be largely determined by the liquid present and the relative rates of the vapour- and liquid-phase reactions. As discussed in Section 4.3.3, below the melting point of Si, the amount of β -Si₃N₄ grown correlates well with the Fe content of the powder, and the proportion of β -Si₃N₄ commonly found in commercial RBSN is consistent with this.

That liquid-phase reactions are dominant in the formation of β -Si₃N₄ is contrary to the view, expressed elsewhere [76, 92], that β -Si₃N₄ may develop from a vapour-phase reaction involving Si and N₂. Such views seem to stem from the unacceptable assumption that the dominant α -Si₃N₄-forming reaction is between SiO and N₂.

It has been argued [89] that the formation of β -Si₃N₄, at a temperature below the Fe/Si eutectic, is indicative of its formation in the absence of liquid. Although, for the reasons outlined above,

some β -Si₃N₄ growth will be formed in the absence of liquid, it is significant that there is evidence of local melting in a commercial silicon powder following argon-sintering at 1150°C [65], that is, below the Fe/Si eutectic temperature.

In addition to the major processes, the following less important effects deserve consideration. Although under normal nitriding conditions the SiO/N₂ reaction is not significant, it might become so when nitridation of volatilized native SiO₂ (Section 4.4.1.7) in the very early stages of the reaction could lead to the observed [45, 47, 90] α -Si₃N₄ whisker growth.

Changes in O₂ and H₂O contents and flow rates of the nitriding gas also influence processes. A p_{O_2} of less than 5×10^{-3} atm in the nitrogen would have little effect on nitridation (Fig. 3, Table III and [76]). It would lead to an increase in p_{SiO} within the compact, but since this cannot be nitrated, it is of little consequence. Rate of diffusion of the SiO from the compact, with consequent weight losses, will depend upon conditions existing at the compact/nitriding gas boundary (Section 4.3.3 and Fig. 7b). At a p_{O_2} higher than 5×10^{-3} atm oxidation of the compact would proceed to such an extent that SiO₂ would form on the Si particles thus preventing their nitridation.

Addition of H₂O will affect the course of the reaction since not only is SiO generated but its nitridation is assisted by the parallel formation of H₂ (Section 4.4.1.4). An enhanced rate of formation of α -Si₃N₄ whiskers would, therefore, be expected. The data (Fig. 3, Table III and [76]) confirm the enhanced rate of formation of α -Si₃N₄, but as far as the growth morphology is concerned there is no definite confirmation. As in the case of the O₂ additions, above a critical p_{H_2O} , SiO₂ will form in the compact, although in this case the situation is complicated by the possible accumulation of H₂.

The diffusion of gaseous contaminants into the compact and of reaction products out, together with parallel nitridation reactions, are responsible for the observed gradients in density and phase composition and for overall α/β ratio [54, 75, 76, 89, 93]. These transport processes will be a complicated function of compact size, geometry, changing permeability, gas-phase composition and flow rate past the compact*. The

* An attempt by Dr J. H. Merkin, Department of Applied Mathematics, University of Leeds, is currently being made to model mathematically some features of a nitriding compact.

novel experimental approach by Lin [94] might offer a means of systematically studying what is, undoubtedly, an extremely complex situation.

Increasing interest is being shown in making additions of H₂ to the nitriding gas, the major effect of which is outlined below. Under typical nitriding conditions, where O₂ and H₂O may well be present in amounts up to 1000 ppm, the p_{SiO} inside the compact would probably be in the range 10⁻⁵ to 10⁻³ atm, that is, 2 to 4 orders of magnitude higher than p_{Si} . With added hydrogen the SiO/N₂ reaction will, therefore, proceed at a fast rate compared to the Si vapour/N₂ reaction and to the β -Si₃N₄-forming reactions (Section 4.4.1.4). The result is the exceptionally fast reaction rate (Fig. 12), high α/β ratio and changed microstructure, compared with those for RBSN made normally [95].

4.6. Interpretation of various experimental data in terms of the model

We now consider miscellaneous nitridation data obtained in the course of various studies and which can be partly rationalized in terms of the model. Since the data were not obtained specifically to test the model, adequate control was not exercised over what would now be regarded as significant variables. Nevertheless, the general trends in behaviour are clear.

Fig. 12 and Table IV show hitherto unpublished [158] kinetics and other data relating to two commercial-type powders nitrided under various conditions. Both powders were derived from the same ingot material but ground differently. The first (Table IV), ground in a steel mill, is typical of that used to obtain much of the published data relating to RBSN. The other powders were ground in a porcelain mill with

alumina grinding media. The different Fe contents reflect the different grinding operations.

The overall reactivities of the two powders is not very different, the specially ground powder reacting the faster (curve 2) almost certainly because of a smaller measured mean particle size. The long linear part of curve 1 is thought to reflect reactions promoted by the Fe-rich liquid phase.

Two important observations can be made. Firstly, avoiding the introduction of Fe by the milling process need not impair powder reactivity, and, secondly, curves 2 to 4 show that the specially ground powder responded to changes in the pressure of the nitriding atmosphere in a similar way to that shown by the very high purity powders (Section 4.3.2). This implies that in both cases the dominant nitriding mechanisms are similar. It is probable that the powder having the

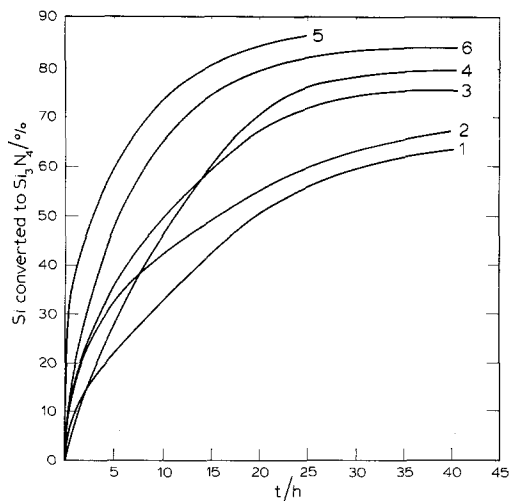


Figure 12 Nitridation kinetics for (1) commercial Si powder, (2)–(6) specially ground Si powder.

TABLE IV Data relating to the nitridation (1350° C) of commercial type silicon powders (cf. Fig. 12)

Curve	% Si reacted	wt % Fe content	% α -Si ₃ N ₄	β -yield (%)*	p_{N_2} (Torr)	p_{H_2} (Torr)
1	63	0.9	83	10.7	760	—
2	67	0.3	73	18.1	760	—
3	75	0.3	75	18.8	200	—
4	80	0.3	84	12.9	50	—
5	96	0.3	84	15.4	720	40
6	85	0.3	85	12.8	95	5

Mean β -yield = 14.8%

*See Fig. 8 for definition.

higher Fe-content would have responded to nitriding gas pressure changes in a similar way, but this was not checked.

Little can be deduced from the β -yield values given in Table IV since the total conversions are so variable. However, it is significant that the mean value of approximately 15% falls within the typical range referred to in Section 4.1 for a commercial Si powder, and is consistent with the Fe content. It has to be appreciated that the form and distribution of the Fe is very different in the two powders and so a simple correlation between amount and β -yield would not be expected.

A more convincing demonstration of the link between liquid-promoting impurities (Fe and Al) and β -Si₃N₄ development is provided by Table V based on data obtained [70] for various commercial RBSN materials and referred to earlier. 5 is exceptional but, as stressed before, there are other α/β -determining variables which have been ignored, principally the nitriding schedule adopted, for which no information is available.

Fig. 13, based on Longland's [56] studies, again illustrates a correlation between liquid and high β -yield. The data for α -forming powder show that high conversions can be obtained with high-purity Si lightly contaminated with Fe; in this special case the Fe is believed to be uniformly distributed over the surface of the particles, encouraging vaporization of Si and high α -yield.

5. The mechanical properties of RBSN

In the previous sections nitridation reactions were discussed, which, together with an appreciation of the mechanical properties of RBSN reviewed below, provide the background for the consideration, in Section 6, of the reaction-bonding process.

An important step in working systematically towards improving mechanical strength of a

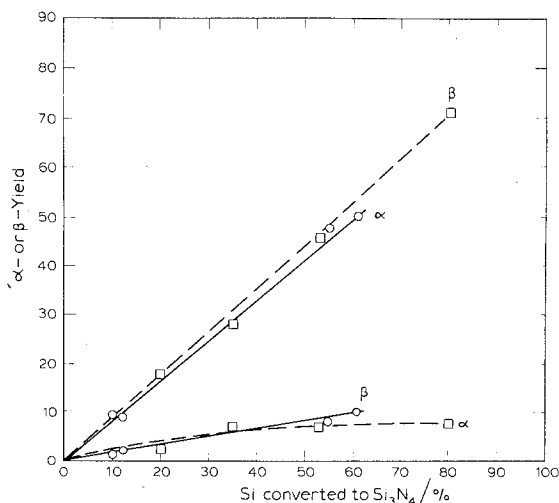


Figure 13 Dependence of α/β ratio on liquid-forming impurity content. \square 98 wt % Si; 1.45 wt % Al; 0.3 wt % Fe; 1370° C, 760 Torr N₂. \circ High purity Si; 200 ppm Al; 40 ppm Fe; 1370° C, 50 Torr N₂ (the low pressure avoiding early inhibition of the reaction).

material is identification of the critical defect, a microstructural inhomogeneity, such as a pore, an inclusion or a microcrack. The methods used to accomplish this have their origins in the work of Inglis [96], Griffith [97] and Sneddon [98]. This led to the equation for the stress (σ_c) necessary to extend a penny-shaped, sharp-fronted crack of radius a , in a material subject to uniform stress normal to the plane containing the crack, namely

$$\sigma_c = \frac{\pi^{1/2}}{2} \left(\frac{2\gamma_i E}{a} \right)^{1/2} \quad (16)$$

in which γ_i is the effective surface energy for fracture initiation and E is Young's modulus of elasticity.

This critical flaw theory has subsequently been developed, initially by Irwin [99], into "fracture mechanics", with the introduction of the material parameters K_{IC} , the critical stress intensity

TABLE V Nitridation data for various silicon powders (after Metcalfe [70])

	Si powder compaction method	Chemical analysis of RBSN			α/β
		Fe	Al	Fe + Al	
1	Iso-pressed	0.79	0.43	1.22	2.4
2	Iso-pressed	0.48	0.43	0.91	2.2
3	Iso-pressed	0.50	0.50	1.00	3.8
4	Iso-pressed	0.54	0.50	1.04	2.6
5	Iso-pressed	0.74	0.21	0.95	0.56
6	Slip-cast	0.51	0.40	0.91	2.4
7	Flame-sprayed	2.0	2.0	4.00	0.3

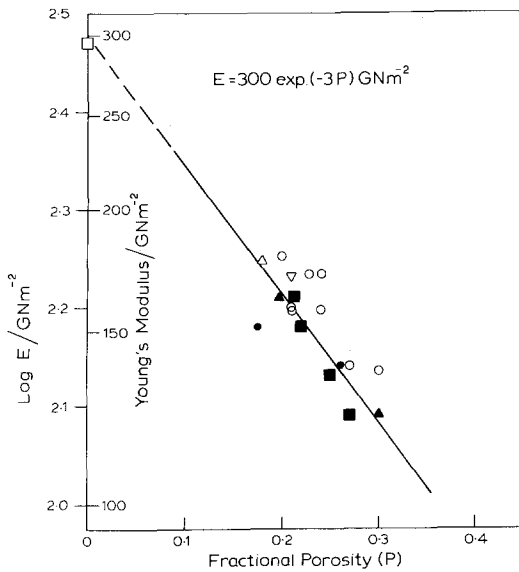


Figure 14 Young's modulus versus fractional porosity. □ mean of 25 values for HPSN [106]; ○ various values [106]; △ high purity RBSN [107]; ▽ Jones *et al.* [90]; ● Dalglish and Pratt [6]; ▲ Evans and Davidge [47]; ■ Barnby and Taylor [117].

factory, and G_c , the critical strain energy release rate. These parameters, which are inter-related, are frequently referred to in the literature on the mechanical properties of RBSN, and full discussions of them are given elsewhere [100–104].

An assumption implicit in methods used to identify the critical defect is that the material properties at the tip of artificially introduced cracks and notches, which are extended under known stresses to determine the fracture mechanics parameters, are identical with those surrounding the actual strength-limiting defect. This is a reasonable assumption for homogeneous materials such as metals and some ceramics, but of doubtful validity for typical RBSN.

5.1. Young's modulus of elasticity

An examination of the literature reveals, not unexpectedly, considerable spread in values of Young's modulus for RBSN. The modulus of elasticity of a material will generally depend upon the amounts and distribution of the phases present but, unlike strength, will be insensitive to sample surface conditions, and to the chance occurrence of relatively large-scale internal defects. In the case of RBSN, however, different processing can lead to different microstructures, and this would be reflected in the values of Young's modulus. It

must also be recognized that when Young's modulus is quoted for RBSN, it is assumed that the phase composition comprises only Si_3N_4 and porosity, i.e. it is fully reacted. Published micrographs leave little doubt that this is not the case and unreacted material must, in part, be responsible for variability.

For these reasons, published data can only indicate trends, and that is all that is claimed for Fig. 14. Here the values are shown plotted on the assumption that they can be fitted to a relationship of the Ryshkewitch–Duckworth [105] type, namely

$$E = 300 \exp(-3P) \text{GNm}^{-2} \quad (17)$$

In drawing the line, two points have been given overriding weight; the value of 300GNm^{-2} which is close to the mean of 25 values compiled by Eddington *et al.* [106] and the value derived from data obtained by Longland and Moulson [107]. The reasons for giving overriding weight to the latter is that it was for an RBSN made from very high purity silicon, and that its microstructure was simple, comprising only dense Si_3N_4 and pores [56, 107]. An additional argument in favour of the procedure adopted is that the other data straddle the line in a reasonable way.

The exponential form of Equation 17 has been criticised on the grounds that it does not meet the physical boundary condition $E = 0$ at $P = 1$. However, Rice [108] regards the principles underlying its derivation as basically sound, and has extended the theory to embrace the entire porosity range. The exponent coefficient in Equation 17, namely 3, is not inconsistent with the amount and type of porosity characteristic of RBSN.

For a comprehensive discussion of the dependence of the mechanical properties of ceramics on microstructure, the reader is referred to the recent review by Rice [109].

5.2. Strength at room temperature

The measured strength of a ceramic is determined in part by the material property and in part by specimen geometry and surface finish. Also, loading rate, loading geometry and nature of the ambient need to be considered. These matters are fully discussed in the literature and it is only necessary here to emphasize that data for RBSN are frequently reported without specification of test conditions.

The situation with RBSN is further complicated because the material property may well be a function of distance from the as-nitrided surface [54, 75]. Dalglish [81] found that grinding removed strength-controlling defects from the as-nitrided surfaces, resulting in strength increases of 45%. Following a similar procedure, Washburn and Baumgartner [110] measured a 17% increase, and Godfrey and Lindley [111] a 55% increase, although no such effects were observed in later studies [90, 112]. Messier and Wong [113] suggest that whether or not surface grinding affects strength depends upon the particle size characteristics of the starting silicon powder.

The Weibull modulus (m) too can be sensitive to surface finish. For specimens with as-fired surfaces, typical values of m are in the range 14 to 18, with higher values (~ 25) measured for specimens having diamond-ground surfaces [7].

Evans and Davidge [47] observed an apparent correlation between strength and α/β ratio in that material with high α/β (~ 4) was about 35% stronger than material with relatively low α/β (~ 0.25). However, very different, two-stage nitriding schedules were adopted in order to vary the α/β ratio, so it is not possible to relate the differences in strength to different nitride phase

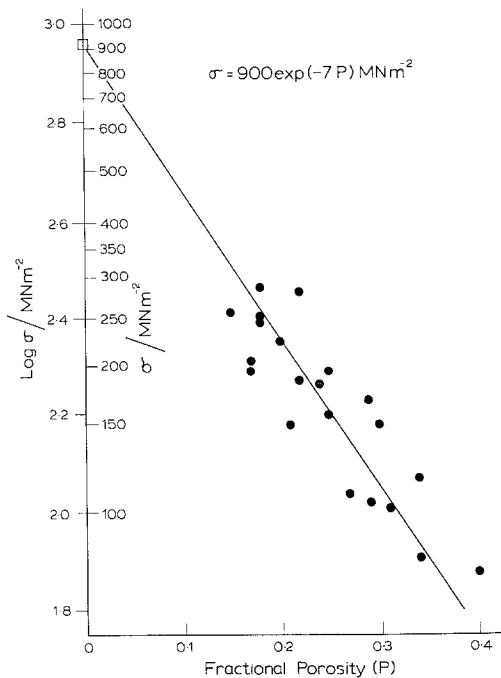


Figure 15 Modulus of rupture versus fractional porosity. All data taken from Eddington [106]. □ HPSN; mean of 40 values; ● various RBSN.

composition, *per se*. Dalglish and Pratt [6] found strength to be independent of α/β ratio.

Although, because of the many variables involved, an attempt at detailed rationalization of room temperature strength data would be unproductive, the following generalizations can be made. There is a dependence on porosity, and Fig. 15 shows data from the literature [106] plotted according to the simple exponential form used previously [114]. The line is described by the following equation:

$$\sigma_c = 900 \exp(-7P) \text{ MN m}^{-2}. \quad (18)$$

Least squares analysis of the data was not made because the weighting to be given to the various values is unknown. For this reason the line was drawn by giving overriding weight to the value for the hot-pressed material, and adjusting the slope to make an apparently balanced pass through the other points: the advantage of the simple constants was a minor consideration.

The plot indicates that, after taking its porosity into account, the strength of RBSN is consistent with that of HPSN.

At this stage an observation might be made relating to the combination of Equations 17 and 18 which leads to the following relationship for the strain at failure (ϵ_c):

$$\epsilon_c = 3 \exp(-4P) \quad (19)$$

This indicates that ϵ_c is $\sim 0.3\%$ for the dense HPSN and $\sim 0.1\%$ for a RBSN for which $P = 0.25$. Ceramics usually fail at a strain of $\sim 0.1\%$ [115], and the underlying physics of the reason for Equation 19 merits examination.

In addition to the clear relationship shown in Fig. 15, there are important trends as exemplified in the results of Dalglish and Pratt [6] on which Table VI and Fig. 16 are based. These show that, apart from the expected dependence upon powder compaction pressure, high mechanical strength would appear to be associated with:

- (i) Si powder of small particle size, and
- (ii) low nitriding temperatures.

In the following section, an attempt is made to rationalize these observations in terms of the dependence of critical defect size on Fe impurity and on processing.

5.3. The critical defect in RBSN

Evans and Davidge [47] first suggested that the

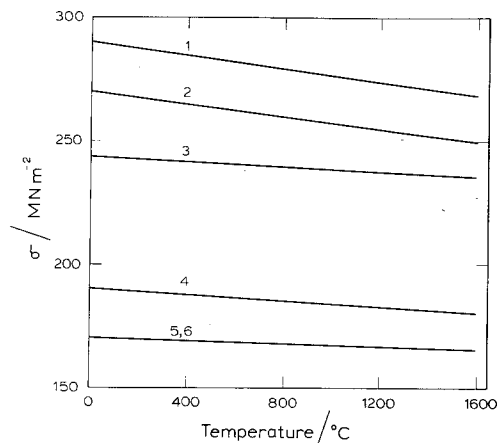


Figure 16 Modulus of rupture versus temperature (after Dalglish and Pratt [6]).

critical defect, which they estimated to be $\sim 25 \mu\text{m}$, was a pore formed as a result of the melting of a large Si particle. Godfrey and Lindley [111] and Godfrey [116] regard the large ($\sim 200 \mu\text{m}$) regions which appear “nebulous” when viewed under “crossed polars”, as meriting serious consideration as strength-controlling defects. Barnby and Taylor [117] estimated the size of the critical defect to be $\sim 400 \mu\text{m}$ and its possible identification with a number of closely spaced pores, or with a region of surface machining damage.

Although there is no consensus concerning its size, and little regarding its nature, there does seem to be general agreement that the critical defect can be caused by local melting. This view is summarized by Dalglish and Pratt [6] as follows: “The strength of reaction-bonded silicon nitride is determined by the size of the largest pores present, i.e. those inherent in the original silicon compact, or those formed as a result of silicon melting at temperatures $> 1410^\circ\text{C}$ ”. Mangels [118] and Wong and Messier [119] express similar views and, because they regard the exothermic nature of the reaction as a principal factor affecting strength, have designed multistage nitriding temperature schedules to reduce the risk of overheating.

While it is important to control the nitriding process so that exotherm effects do not cause melting, there is now strong evidence that the major cause of large defects is Fe contamination.

Marked changes in the microstructures of

“green” silicon compacts have been observed [65, 120] following Ar-sintering in the range 1150 to 1250°C , i.e. under conditions in which exotherm effects do not arise. There was clear evidence of local melting which was undoubtedly associated with Fe particles. It has since been confirmed [121] that the impurity is introduced during milling of the typical commercial powders.

During Ar-sintering, or at the beginning of the nitriding process, this adventitious Fe reacts with the Si to form a liquid, which migrates into the microstructure leaving a pore at the site of each Fe particle. As nitridation proceeds, those parts of the compact contaminated with Fe develop into the “microstructural inhomogeneities” typical of RBSN, namely voids, usually $\sim 20 \mu\text{m}$ diameter, surrounded by a dense region of mainly $\beta\text{-Si}_3\text{N}_4$. The dense region is typically of diameter 50 to $100 \mu\text{m}$, but the microstructure can be influenced over regions of up to 1 mm diameter [65]. It also seems likely that the Fe contamination and the “nebulous” regions [111, 116] are related, the optical scattering being caused by $\alpha\text{-Si}_3\text{N}_4$ whiskers formed at the outset of the reaction (Sections 4.4.1.7 and 4.5).

In the light of these observations, the trends in Table VI and Fig. 16 can be interpreted as follows. The fine powder ($3 \mu\text{m}$) was obtained from as-received powder by elutriation, a process which also reduced the Fe content. It is probable, therefore, that low Fe content and the elimination of large Fe particles might be the indirect cause of the improved strength, and the absence of large voids in the corresponding micrograph in Fig. 17 is consistent with this.

Niwano and Moulson [66] observed a similar segregation of Fe accompanying air-classification of a specially ground* powder into various size fractions, as Table VII shows, the classifier treating the denser Fe-bearing particles as relatively large Si particles.

As the nitriding temperature is raised, the Fe/Si melt will move out further into the surrounding microstructure, as the average Fe/Si compositions follow the liquidus in the silicon-rich direction [34]. Therefore, since the size of the Fe-induced defect would increase with temperature, the strength would correspondingly decrease. Con-

* Note that contamination with Al_2O_3 would be expected from the milling and that similar segregation appears to have taken place.

TABLE VI Nitridation data for various silicon powders

Curve no. (Fig. 16)	Mean particle size of Si powder (μm)	Fe-conc. (wt %)	Compaction pressure (MN m^{-2})	Nitriding schedule	ρ_n (kg m^{-3})
1	3	< 0.1	345	L	2610
2	3	< 0.1	345	H	2610
3	8	< 0.4	345	L	2630
4	8	< 0.4	345	H	2630
5	3	< 0.1	69	L	2350
6	3	< 0.1	69	H	2350

L: 84 h at 1330° C + 15 h at 1450° C

H: 12 h at 1330° C + 36 h at 1450° C

(after Dagleish and Pratt [6]; Fe contents from [81]).

TABLE VII Chemical analyses (wt %) of air-classified size fractions of specially ground (porcelain mill with Al_2O_3 grinding media) commercial Si ingot (after Niwano and Moulson [66]).

E	As-milled powder	Size-classified fractions				
		> 20 μm	20–10 μm	10–5 μm	5–2.5 μm	< 2.5 μm
Ti	0.12	0.14	0.08	0.09	0.10	0.03
Al	0.99	1.00	0.95	1.04	0.88	0.75
Fe	0.31	0.46	0.40	0.35	0.28	0.22
Ca	0.06	0.06	0.05	0.06	0.05	0.07
Mg	0.01	0.01	0.01	0.02	0.02	0.02
Mn	0.02	0.02	0.02	0.02	0.01	0.01
K	0.03	0.03	0.02	0.05	0.04	0.04
Na	0.02	0.03	0.02	0.04	0.03	0.03

TABLE VIII Fabrication details (cf. Fig. 18)

Reference	Si powder				Nitriding process	ρ_n (kg m^{-3})	α/β
	Particle size	Chemical analysis (wt %)					
		Ca	Al	Fe			
[128]	8–9 μm mean size	0.15–0.30	0.25–0.50	0.4–0.6	N_2 : commercial production schedule (AJM assumes it would be 2-stage; part below and part above 1420° C)	2460–2590	1.0–1.5
[114]	Commercial Si powder (2 wt % impurities): same source as that of powder used by Noakes & Pratt [128].				N_2 : schedule varied to give “predominantly $\alpha\text{-Si}_3\text{N}_4$ ” or “predominantly $\beta\text{-Si}_3\text{N}_4$ ”	2600	–
[95]	325 mesh	0.02–0.8	0.4–0.6	0.66–0.75	N_2 : 2-stage schedule 36 h at 1260° C 24 h at 1460° C	2300	1.5–2.3
[95]	325 mesh	0.02–0.8	0.4–0.6	0.66–0.75	1% H_2 + N_2 Same 2-stage schedule as above	2300	1.5–2.3
[110]	No details available						

versely, the lower the nitriding temperature the smaller will be the inhomogeneity and the higher the strength.

Furthermore, the observation by Elias *et al.* [89] that low strengths are always associated with high β - Si_3N_4 contents is not unexpected, although the correlation might not be with β - Si_3N_4 itself but with the Fe (Section 4.3.3).

The hypothesis that Fe impurity leads to strength-limiting defects in commercial RBSN rests on circumstantial evidence. Direct evidence could be obtained through fractography, and it is unfortunate that, for RBSN, the topic appears to have received little attention. The identification of fracture origins in RBSN, though challenging, should be undertaken if the mechanical properties of the material are to be optimized in a systematic way. Where illustrations of fracture surfaces have been reported [81, 6, 70] they contain large voids which, from their appearance, seem to have been formed in the way described by Arundale and Moulson [65].

Jones *et al.* [90] regard the critical defects as intrinsic to the microstructure of RBSN rather than impurity induced, and cite the linear strength/partially nitrided density relationships (Section 6) to support their argument. On the other hand, the following qualitative argument can be advanced to reconcile the relationships with Fe-induced critical defects.

If, in Equation 16, γ_i and E increase in proportion to nitrided density, with a remaining constant, then it follows that σ_c will vary linearly with extent of nitridation, as observed. It is known that E does vary in the required way [90, 107] and, from the earlier arguments, a is likely to remain sensibly constant. Nothing is known of γ_i in the region of an Fe-induced inhomogeneity, but it is reasonable to suppose that it would increase with nitrided density ([109], p.236). The departure from linearity observed [90] for a powder having exceptionally high ($>1.0\%$) Fe content could result from defect interaction [122].

Finally, a small addition of H_2 to the nitrogen has a marked effect on mechanical properties, and this requires explanation. It has been shown (Section 4.4.1.4) that SiO nitridation is promoted by H_2 additions; the rapid active oxidation of the Fe-contaminated zones, along with the rest of the silicon, and nitridation of the SiO generated, would lead to the observed finely textured and relatively void free microstructure [95].

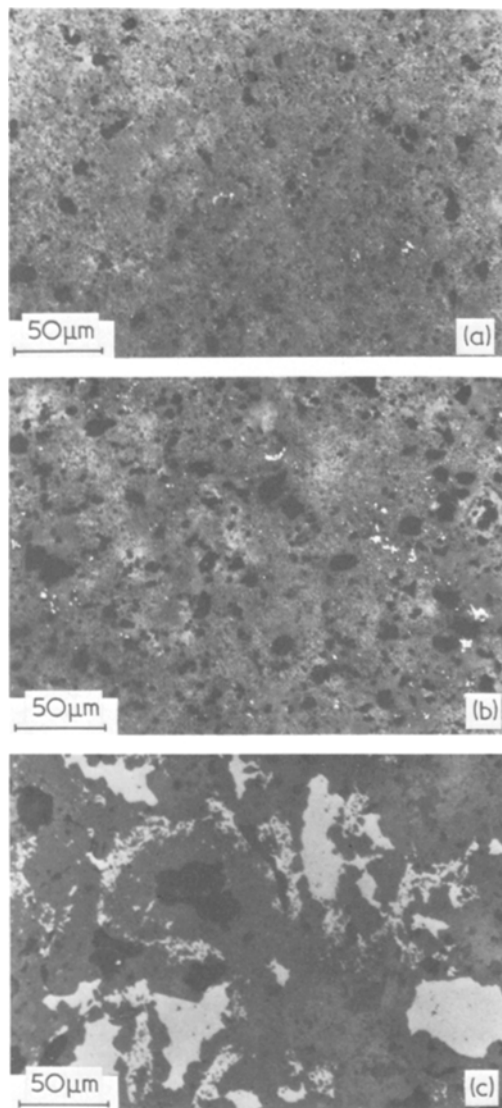


Figure 17 Optical micrographs of reacted materials (nitriding schedule L: cf. Table VI and Fig. 16). (a) for "Curve no. 1": $< 0.1\% \text{Fe}$; (b) for "Curve no. 3": $< 0.4\% \text{Fe}$; (c) for coarse fraction; mean particles size $\sim 30 \mu\text{m}$; $\text{Fe} < 0.5 \text{ wt}\%$ (after Dalglish [81]).

5.4. Strength at high temperatures

High temperature bend strength data are shown in Fig. 18 and fabrication process details given in Table VIII. Resistance to creep is critical in the engineering application of RBSN and a target for its acceptance for some components in a vehicular gas-turbine is less than 0.5% total strain after 200 h at 1260°C under a tensile stress of 70 MN m^{-2} [123].

An excellent discussion of the creep properties of RBSN is given by Grathwohl and Thümmeler [124] who demonstrate the overriding impor-

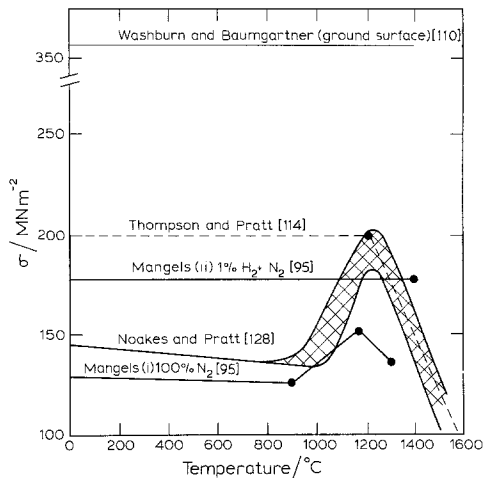


Figure 18 Various high-temperature strength data.

tance, in determining creep, of oxidation processes occurring in the interior of RBSN (“internal oxidation”), following ingress of oxygen via the pore system of the ceramic. Internal oxidation of RBSN is inhibited through the blocking, by oxide, of channels leading from the specimen surface to the interior. Whether or not such channels can be effectively blocked depends upon their radii, and Grathwohl and Thümmeler conclude that RBSN having pore radii mainly below 0.04 to $0.05 \mu\text{m}$ behave satisfactorily in this respect. They correlate tendency to creep with pore size distribution, the least creep resistant material being characterized by having a broad distribution around a mean size of approximately $0.2 \mu\text{m}$ and the most creep resistant having a narrow distribution about a mean of approximately $0.03 \mu\text{m}$.

Mangels [123, 95] and Ud Din and Nicholson [125] attribute creep to relative grain movement facilitated by a grain-boundary glassy phase, and Ca and Al are believed to have an adverse effect on creep resistance since they would lower the viscosity of this glass. The internal oxidation observed by Grathwohl and Thümmeler would be the precursor to grain-boundary oxidation.

Mangels showed that a small addition of H_2 to the nitriding gas (N_2) led to a material having much improved creep characteristics. This improvement might be a consequence of the evaporation or redistribution of the impurities, or of better oxidation resistance associated with a finer textured microstructure.

As far as the author is aware, the possibility that Fe might affect creep properties has not been considered. It may be significant, though, that the

data obtained by Grathwohl and Thümmeler show a qualitative correlation between broadness of pore size distribution (and so tendency to creep) and Fe content.

It has been suggested that $\alpha\text{-Si}_3\text{N}_4$ is inherently more creep-resistant than $\beta\text{-Si}_3\text{N}_4$ [114] but the experimental basis for this suggestion needs re-examination in the light of the more recent work. It is probable, for instance, that the processing required to control the α/β ratio could also change grain-boundary content and composition. Similar changes might also be responsible for the observation by Parr *et al.* [126] that a 5 wt% addition of SiC powder to the Si led to improved creep properties.

The increase in strength at about 1200°C (Fig. 18) could also be related to grain-boundary glass, and is probably a reflection of the increase in γ_{F} observed by Coppola *et al.* [127] in the same temperature region. As might be expected, no similar increase in strength is observed in material fabricated with H_2 added to the nitriding gas.

5.5. Effective surface energy for fracture initiation at room temperature

Evans and Davidge [47] estimated γ_{i} from the stress required to extend artificially introduced, sharp-fronted, cracks. They obtained a value of 6 J m^{-2} ($\rho = 2550 \text{ kg m}^{-3}$), which was insensitive to α/β ratio and to pore size and size distribution. A lower value, 4 J m^{-2} , was measured for lower density material ($\rho = 2130 \text{ kg m}^{-3}$).

Barnby and Taylor [117] determined K_{IC} values from the stress required to extend both natural, sharp-fronted cracks and machined notches of radii in the range 120 to $>1500 \mu\text{m}$. They found a tendency for measured K_{IC} to increase with notch radius and concluded that the narrow machined notches ($120 \mu\text{m}$) behaved as sharp-fronted cracks. They estimated a value for γ_{i} of approximately 30 J m^{-2} .

Dalgleish and Pratt [6] measured the same value for γ_{i} of approximately 30 J m^{-2} for notches of radii 320 , 160 and $80 \mu\text{m}$. For notches of radius $20 \mu\text{m}$, and for sharp-fronted cracks, they obtained a value of approximately 10 J m^{-2} for γ_{i} ($\rho = 2610 \text{ kg m}^{-3}$) and a lower value of 7 J m^{-2} for less-dense material ($\rho = 2350 \text{ kg m}^{-3}$). Jones *et al.* [90] measured values for γ_{i} in the range 9 to 14 J m^{-2} for partially nitrided material (ρ in the range 2300 to 2500 kg m^{-3}).

In all studies, except those of Dagleish and Pratt [6], the silicon powders were of “commercial” type; from information given elsewhere [81] the powder used by Dagleish and Pratt is estimated to have contained ~ 1 wt% total cation impurity. Because of this, the possible influence of large Fe-induced voids and microstructural inhomogeneities on measured γ_i cannot be ignored. For instance, on the basis of an, albeit, oversimplified argument the following plausible explanation for the difference in γ_i values determined from the extension of sharp-fronted cracks on the one hand, and relatively blunt notches on the other, can be offered.

A normal commercial silicon powder contains about 1 wt% Fe, and assuming the Fe particles, or Fe-bearing particles, have a mean size the same as that of the Si particle ($\sim 15 \mu\text{m}$), and to be three times as dense, they will be spaced, on average, about $100 \mu\text{m}$ apart. As indicated, then, in Fig. 19, a sharp crack will almost certainly miss an inhomogeneity, whereas in the case of a notch of radius greater than approximately $20 \mu\text{m}$, there is a large chance that one will lie in the notch root surface.

From the previous discussion (Section 4.4.1.6), and from the appearance of the microstructure surrounding the void shown by Dagleish and Pratt [45], it could reasonably be argued that the K_{IC} value for the contaminated zone might be higher than that for the background material. At the very least it is likely that the complex, inhomogeneous microstructure encountered in the region of the larger radius notch root would influence the stress necessary to initiate fracture.

In this context the observation by Thompson and Pratt [114] that “the fracture path showed

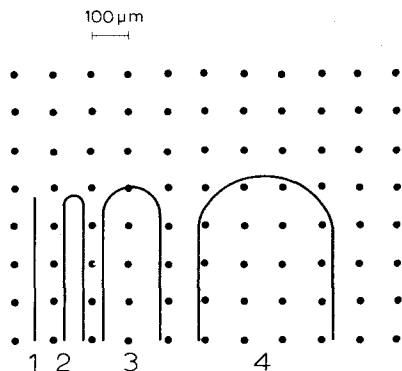


Figure 19 Schematic illustration of the distribution of Fe-induced defects with respect to machined notches. (1) sharp-fronted crack; (2) notch radius $20 \mu\text{m}$; (3) notch radius $80 \mu\text{m}$; (4) notch radius $160 \mu\text{m}$.

some cleavage of the dense grains, but generally followed the low-density regions” is worthy of note. The dense regions would reasonably be identified with the dense Fe/Si melt-out zone referred to earlier (Section 5.3).

The literature to date indicates that carefully designed experiments, on well-defined material, must be carried out before γ_i values representing an intrinsic material property of RBSN can be accepted with confidence. This opens to question the validity of using currently available K_{IC} values to estimate the size of the critical defect.

6. The reaction-bonding process

In discussing the reaction-bonding mechanism it is necessary to consider separately two types of nitriding atmosphere, namely nitrogen, and nitrogen with added hydrogen. It will also be helpful to discuss the topic in three parts: the first describing general observations concerning the development of the mechanical properties as the nitriding reaction proceeds; the second describing what is known of the bonding mechanism in the absence of the impurities present in “commercial” silicon powder and the third with studies on commercial type powders.

6.1. General observations

Jones and Lindley [129] observed a linear relationship between the developing bend-strength (σ_c) of the ceramic during nitridation, and the partially nitrided compact density (ρ_n). They also demonstrated that σ_c was sensibly independent of the “green” compact density (ρ_g). At first sight this latter observation is surprising because the implication is that for two compacts to have the same σ_c value, they need only have the same ρ_n value; the fact that essentially they might be three-phase composites comprising very different amounts of the various phases being of minor significance. Fig. 20 shows a typical linear relationship and Table IX phase compositions before and after nitriding of, respectively, “high” and “low” ρ_g compacts:

The phase compositions can be readily calculated using the following relationships:

$$C_p = 1 - 0.281\rho_g - 0.148\rho_n \quad (20)$$

$$C_{Si} = 1.072\rho_g - 0.643\rho_n \quad (21)$$

$$C_{SN} = 0.791(\rho_n - \rho_g) \quad (22)$$

in which C_p , C_{Si} and C_{SN} are, respectively, the volume fractions of porosity, silicon and silicon

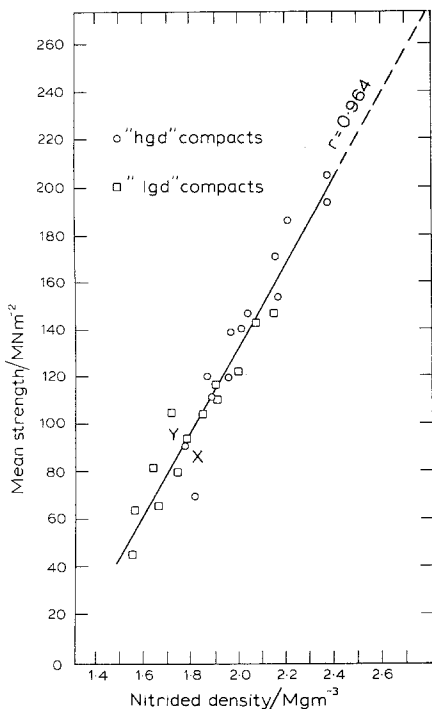


Figure 20 Strength versus nitrided density for "high" (hgd) and "low" (lgd) compacts (after Jones and Lindley [129]).

nitride. It is perhaps significant that, although in Table II the phase compositions differ considerably in the amounts of Si and Si_3N_4 , there is only a small difference in fractional porosities.

Jones and Lindley argue that, because the three major strength-determining parameters (Equation 16), E , γ_i and c would be expected to be different for two compacts having different phase compositions, their observations implied that "there exists a subtle relationship between E , γ_i and c and the structure of the partially nitrided compacts, differences in one parameter between the two materials being compensated for by corresponding differences in one or both of the other parameters". Because different silicon powders exhibit their own particular straight line σ_c/ρ_n relation-

TABLE X Dielectric property data for RBSN

$\rho \text{ kg m}^{-3}$	Frequency (GHz)	Relative permittivity	$\tan \delta$	Reference
~ 2300	9-12	6.17	0.017	[138]
2500	8.52	5.54	0.0036	[139]
~ 2500	9.8	5.6	0.002	[137]
2556	9.37	5.92	0.006	[140]
2240-	10.0	4.98-	0.008-	[141]
2490		6.15	0.004	

ships, it was argued that such relationships could simplify the approach toward optimizing the mechanical properties of RBSN.

It was further shown [93] that mechanical strength could be sensitive to the precise nitriding conditions. In particular, σ_c depended upon whether the nitriding gas (N_2) was in a "static" condition around the samples or whether it flowed past them. On the other hand, whereas additions of O_2 and H_2O to the nitriding gas might influence the nitriding reaction, their effect on strength was of no practical significance until additions as high as ~ 1 vol % were enough to cause the formation of $\text{Si}_2\text{N}_2\text{O}$ and SiO_2 [76].

As far as identification of the bonding mechanism and of the strength-controlling defect were concerned, there was no firm knowledge. It was generally assumed, largely on the basis of the arguments mentioned in Section 4.2, that the bonding involved the steady development of an $\alpha\text{-Si}_3\text{N}_4$ whisker mat, and that the weakest links in the structure were voids formed by the melting of the largest silicon particles remaining when the nitriding temperature was taken above the melting point of silicon [47].

6.2. Studies using high-purity Si powders

Longland and Moulson [107] studied development of Young's modulus during nitriding of specially prepared [42] high-purity Si powder with the aim of understanding the mechanism of the reaction-bonding process. It was believed that, from such an understanding, there could be a logical progression towards the elucidation of bonding processes during nitridation of the chemically more complex Si powder compacts.

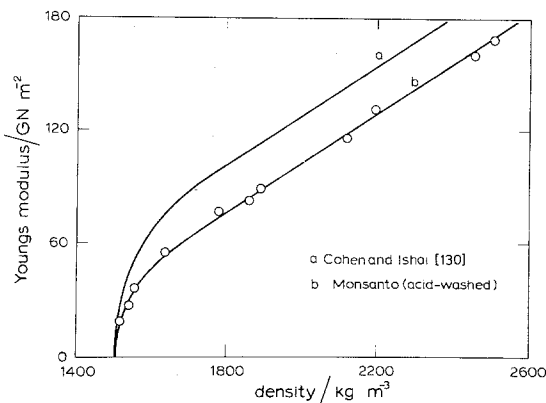


Figure 21 Theoretical (a) and experimental (b) E/ρ_n data (after Longland and Moulson [107]).

Fig. 21 shows that a well-defined linear relationship exists between E and ρ_n , similar to those observed for the reaction-bonding process starting with the less pure commercial Si powders [90]. This suggests that the bonding mechanism is similar in the two cases.

A satisfactory description of the rate of development of E with ρ_n is provided by the three-phase composite model developed by Cohen and Ishai [130]. This leads [107] to the following equation for Young's modulus of the porous Si_3N_4 -Si composite ($E_{\text{PSN-Si}}$) in terms of the modulus for Si_3N_4 (E_{SN}) and the phase composition of the composite:

$$E_{\text{PSN-Si}} = E_{\text{SN}} \left[1 - \left(\frac{C_p}{1 - C_{\text{Si}}} \right)^{2/3} \right] \times \left[1 + \frac{C_p}{m \left[m - 1 + \left(\frac{C_p}{1 - C_{\text{Si}}} \right)^{2/3} \right] - C_{\text{Si}}^{1/3}} \right]$$

m is the modular ratio, $E_{\text{Si}}/E_{\text{SN}}$, in which $E_{\text{Si}} \sim 100 \text{ GN m}^{-2}$ and $E_{\text{SN}} \sim 300 \text{ GN m}^{-2}$. By substitution of the Equations 20 to 22, the dependence of $E_{\text{PSN-Si}}$ on ρ_g and ρ_n can be found.

Fig. 21 shows that, although the model provides a good description for the rate of development of E with ρ_n , as far as the absolute values of E are concerned, it needs refinement.

The microstructures (Fig. 22) show the nitride phase at a very early, and later, stage of its development. It is clear that "whiskers" play no part in the bonding, and that the morphology of the growth is similar to that of the α - Si_3N_4 growth observed by Guthrie and Riley [131] and of the CVD α - Si_3N_4 deposits [21, 26].

6.3. Studies using commercial Si powders

The view that the bond in RBSN resides in an interpenetrating mat of α - Si_3N_4 was first proposed by Parr and his colleagues [126]. Thompson and Pratt [14], on the other hand, considered the strength of the material to be largely dependent upon the amount of contact between dense grains of Si_3N_4 , with the low-density α -mat regions being the weakest parts of the structure. They based their opinions on their observation of fracture

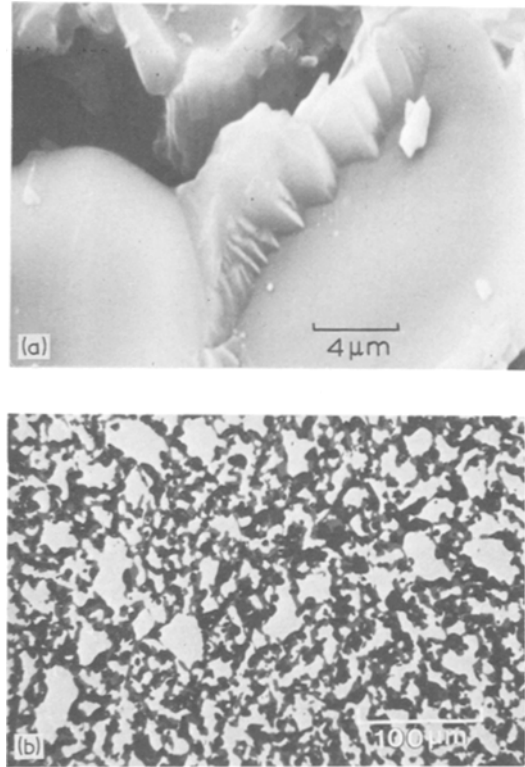


Figure 22 High purity Si powder compact partially nitrided at 1370°C in N_2 at 50 Torr: (a) SEM of nitride growth in neck region after 0.5 h; (b) polished section (optical) showing growth after 3 h and porosity developing in silicon (see also Fig. 5). (After Longland [56]).

paths and on the dependence of E on porosity (Fig. 14), which they considered incompatible with a steadily thickening whisker model.

Recently Jones *et al.* [90], placing strong emphasis on the linear σ_c/ρ_n and E/ρ_n relationships for partially nitrided material, considered that the strength develops through the formation and densification of a whisker mat formed by the vapour-phase nitridation of SiO . However, as shown in Section 6.2, linear E/ρ_n relationships are also observed when whisker growth is absent, and more recent studies [56] have shown that for this high purity material the same seems to apply for the developing strength.

These observations, together with the arguments concerning kinetics and morphology (Section 4.5), must leave the "whisker bond" hypothesis open to question, while supporting the "intergranular bond" model proposed by

Thompson and Pratt [114]. The micrograph by Ud Din and Nicholson [125], showing the apparent separation of grains of Si_3N_4 after high temperature creep, might also be cited in support of an intergranular bond; it is unlikely that such a well-defined grain boundary would be seen were the material to be bonded essentially by a thickened whisker mat.

Although the microporous $\alpha\text{-Si}_3\text{N}_4$, regarded as a characteristic feature of RBSN microstructure, would suggest a whisker mat, it could also be consistent with the deposition of massive $\alpha\text{-Si}_3\text{N}_4$. During the nitriding of commercial Si powders many extrinsic microstructural features would develop, for example VLS needles and whiskers formed in the early stages of the reaction, and these would present a complex substrate for deposition of the pyrolytically formed massive Si_3N_4 . It is likely, therefore, that under such conditions a microporous deposit might be formed rather than the dense material deposited in the geometrically simpler and chemically purer systems.

Even though the developed microstructures may be comparable, only the correct model for their generation can guide future research and development effort reliably.

A different type of bond and microstructure is developed when hydrogen is added to the nitriding gas. In this case the interpenetrating and steadily thickening $\alpha\text{-Si}_3\text{N}_4$ whisker mat does represent a reasonable model for the reasons given (Section 4.5). Also, because the nitridation of SiO is now the dominant reaction, the second-order effects associated with the flow rate of the nitriding gas are no longer observed [132].

7. Summary of a proposed model for the formation of RBSN

(1) In normal nitriding of commercial silicon powder compacts, strength develops through the continuous deposition of massive $\alpha\text{-Si}_3\text{N}_4$, following the vapour-phase nitridation of Si vapour.

(2) Voids and microstructural inhomogeneities occur locally throughout the ceramic as a direct consequence of the melting of Fe/Si alloys formed from the Fe or Fe-bearing particles.

In attempting to control the microstructure of RBSN it is important to appreciate that the pre-

cursors to these defects originate during the Ar-sintering stage and, because of the presence of other impurities, at temperatures as low as 1150°C .

(3) During nitridation, well-formed $\beta\text{-Si}_3\text{N}_4$ crystals grow in the impurity-contaminated zones. The $\beta\text{-Si}_3\text{N}_4$ content of a completely nitrided compact is related to the amount of impurity, through its control of the amount of liquid formed during nitridation.

(4) The strength of the ceramic is limited by the impurity-associated microstructural inhomogeneities. This dominating effect explains why the strength of most commercial RBSN materials is relatively independent of the many differences in processing parameters which will have been encountered.

(5) The addition of H_2 to the nitrogen changes the reaction to one involving the nitridation of SiO , with a corresponding change in the morphology of the nitride from the "massive" CVD $\alpha\text{-Si}_3\text{N}_4$ form to the "whisker" form.

(6) The improvements in mechanical properties associated with the "hydrogen-fired" material have their origin, at least in part, in the redistribution and evening-out of concentrations of impurity. This occurs because the reaction involving SiO proceeds at a much faster rate than that involving Si vapour, the $\beta\text{-Si}_3\text{N}_4$ -forming reaction rate remaining sensibly unchanged.

8. The optical and electrical properties of RBSN

Commercial RBSN has a total porosity of approximately 20% and there is a fine dispersion of unnitrided material distributed throughout the ceramic (Fig. 2). This is usually referred to as "silicon" but will, at least in part, comprise alloys of silicon with iron and, possibly, other cation impurities associated with the starting silicon powder. Therefore, it is not sensible to discuss in any detail the electrical and optical properties of such a heterogeneous material and only reasonable to offer some general observations which help towards an overall appreciation of them.

Because silicon nitride "thin" films, usually regarded as amorphous, find application in semiconductor technology, there is an extensive literature covering their properties which is reviewed by Milek [133]. The band-gap of crystalline Si_3N_4 is

reported to be approximately 4.0 eV, with the optical absorption edge extending over the wavelength range 200 to 300 nm [133]. Since the visible spectrum ranges from approximately 350 to 750 nm, it should be transmitted by bulk Si_3N_4 , and massive CVD Si_3N_4 is transparent [134]; it would be expected, therefore, that polycrystalline Si_3N_4 be white and opaque. While both RBSN and HPSN are opaque they are not white, commercial RBSN being typically dark grey and HPSN nearly black.

The characteristic dark grey colour of commercial RBSN is, in part, due to Fe, and this is apparent from a comparison of the straw colour of materials fabricated from high purity silicon with that of materials made from similar silicon powder but contaminated with small amounts (~ 100 ppm) of Fe from the comminution and size-classification processes [135]. It is possible that the darkening arises as a result of Fe in solution in the Si_3N_4 lattice, in a way similar to that encountered in Fe-contaminated Al_2O_3 [136]; the blackness of HPSN might then be expected because of the severely reducing, hot-pressing conditions, namely 1650°C in a graphite die.

The refractive index of amorphous thin films of Si_3N_4 is approximately 2.0 [133], and it would be reasonable to assume, for the present, the same value for α - and β - Si_3N_4 .

As already mentioned, there has been interest in the dielectric properties of "thin" films of Si_3N_4 for many years, but only recently in those of the ceramic forms. This latter interest has arisen because of the potential use of RBSN in radomes, an application which demands a material easy to fabricate to close dimensional tolerances, with good thermal shock resistance and acceptable dielectric properties [137]. In service, radomes may be rapidly heated by air friction to 500°C in about 30 sec, and current developments require the material to withstand heating to 1000°C in the same time and yet still retain good and controlled transparency to microwave radiation. It is clear why interest is shown in the temperature coefficients of relative permittivity and $\tan \delta$ but, at present, it is not known how they are affected by fabrication variables. It is generally accepted that poor dielectric properties are associated with incomplete nitridation and, since the electrical properties of silicon are so sensitive to very small amounts of cation impurity in solution, it is not

surprising that the literature relating to dielectric losses of "commercial" RBSN presents a confused picture. From the brief discussion of optical properties, it is evident that electrical property data determined for dark grey or black silicon nitride should be treated with caution. However, the situation might improve quickly now that greater interest is being taken in high purity starting powders.

In the context of radome development, the first reference to the microwave permittivity of RBSN was made by Wells [138], although it was not until the early 1970s that an acceptable low $\tan \delta$ (< 0.01) was reported by Westphal and Sils [139]. Since then low values of dielectric loss, summarized in Table X, have been measured by various researchers [137, 140, 141]. Estimates of the relative permittivity for theoretically dense material can be made from data for porous materials using formulae discussed, for example, by Tareev [142].

The temperature coefficient of relative permittivity is found to be approximately 10 ppm K^{-1} [139] but, for materials showing the higher dielectric losses, coefficients ranging from between $+3$ and $+354 \text{ ppm K}^{-1}$ are reported [140]. This type of behaviour is not uncommon in dielectric materials [143] and is likely to be a reflection of strongly temperature-dependent charge transport processes; these are directly responsible for the dielectric losses, with internal polarization against phase boundaries producing the permittivity effects.

Recently, Thorp and Sharif [144] measured the dielectric properties of hot-pressed silicon nitrides and found, at room temperature, a relative permittivity of approximately 9.5 over the frequency range 10^2 to 10^{10} Hz. Relative permittivities for CVD Si_3N_4 of 7.5 to 8.8 at 9.37 GHz have been reported by Perry [145] and, from measurements on thin films, Chu *et al.* [146] estimated a value close to 9.0 (1 MHz).

In summary, then, and to a first approximation, silicon nitride is to be regarded as an insulator having band-gap, refractive index and relative permittivity values of approximately 4.0 eV, 2.0 and 9.0, respectively. More precise values will only become available when careful measurements are made on bulk materials, of well-defined chemical purity and stoichiometry, most probably fabricated by vapour-deposition techniques. As far as RBSN

TABLE IX Phase composition data: cf. Fig. 20 (after Jones and Lindley [129])

Material	Green density (Mg m ⁻³)	"Green" structure		Weight gain (%)	Conversion (%)	Nitrided structure			Nitrided density (Mg m ⁻³)	
		Vol% Si	Vol% pores			Vol% Si	Vol% Si ₃ N ₄	Vol% pores	Theoretical	Measured
"hgd"	1.56	67.0	33.0	12.9	19.3	54.1	15.8	30.1	1.77	1.77
"lgd"	1.34	57.5	42.5	33.3	49.9	28.8	35.3	35.9	1.80	1.78

is concerned, its high porosity will always be a complicating factor.

9. Thermal properties of RBSN

Thermal properties of ceramics are important because, with mechanical properties, they determine characteristic resistance to failure by thermal shock and steady state thermally induced stress. It is mainly for this reason that considerable effort has been devoted to measuring the thermal expansion, diffusivity and conductivity of RBSN. Specific heat has been measured since it is involved in the relationship between thermal diffusivity and conductivity.

Thermal expansion coefficient is a deceptively difficult property to measure accurately, particularly when it is low, as with silicon nitride. In the case of RBSN, the high surface area associated with the fine scale porosity poses additional problems. For example, the author has observed anomalous dimensional changes in the temperature range 20 to 150°C when measuring the thermal expansion of some specimens, a behaviour strongly indicative of moisture adsorption/desorption effects [147, 148]. These difficulties, together with the fact that RBSN is currently not a well-defined material, are in part responsible for the range of values quoted in the literature [138, 149–151] and there is little point in attempting to assign a firm value for the expansion coefficient until careful measurements are made on well-characterized material. For the present the author adopts the value, quoted in Table II, of $3.0 \times 10^{-6} \text{ K}^{-1}$ for the mean coefficient from room temperature to approximately 1000°C.

Conductivity is, perhaps, the most difficult thermal property to measure accurately. This is because there is a factor of only approximately 10^4 in conductivity value between the most conducting and most insulating materials. It is, in consequence, not easy to confine heat flow to any particular predetermined path in "steady state" experimental arrangements, and the problem is

severely aggravated at high temperatures. Added to this is the difficulty in assuring good thermal contact between one material and another, and this requirement is usually a feature of steady state measurement techniques.

For many years the laboratories of the British Ceramic Research Association have been involved both in the development of RBSN and in perfecting techniques for accurate measurement of thermal properties of ceramics. It is for these reasons that the author has drawn exclusively on data from that source.

Fig. 23, showing the variation of specific heat with temperature, is derived from a paper by George [152]; the band embraces his own results and those he obtained from the literature. The form of the curve is what would be expected for solids in general [153].

George also developed a method for measuring thermal diffusivity based on timing the passage of a transient heat pulse through a small disc specimen, following illumination of one face by a laser flash. The thermal diffusivities of ten RBSN materials were measured over the range 300 to 700 K and then transformed to conductivity values by using the measured values of density and specific heat. The materials covered nitrided density and α/β ratio values of 1990 to 2840 kg m⁻³ and 0.1 to 4.0, respectively.

The studies revealed the expected trends, namely for conductivity to decrease with tempera-

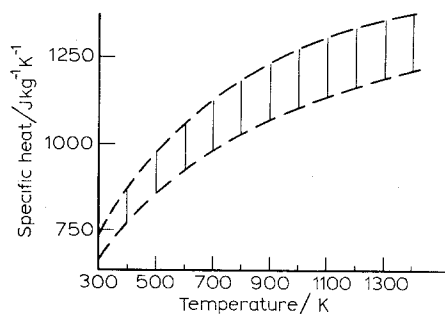


Figure 23 Specific heat of RBSN (after George [152]).

ture and increase with density. The amount and distribution of unreacted material was observed to be a major influence on conductivity.

Later, using the same technique, Barratt and Ruddlesden [154] extended conductivity measurements to 1000°C. Fig. 24 shows their data for a typical RBSN made from a commercial silicon powder.

As in the case of the other properties of RBSN, a reliable correlation between thermal properties and other material parameters will have to await the availability of well-defined and characterized material.

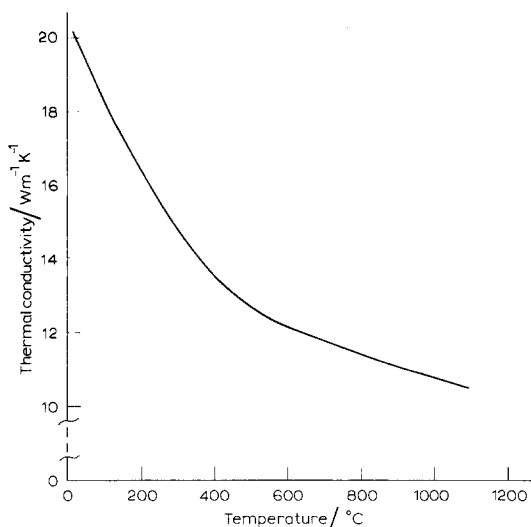


Figure 24 Thermal conductivity of a RBSN (commercial Si; weight gain on nitriding = 64.66 wt%; $\rho_n = 2560 \text{ kg m}^{-3}$) (after Barratt and Ruddlesden [154]).

10. Suggested further research and development work

From this review, lines along which research and development work might profitably be extended may be identified. It is convenient to separate them into those concerned with the science of the fabrication and properties of RBSN, and those more directly concerned with the development of a better material.

10.1. Basic science relating to RBSN

(1) There is need for data on mass and charge transport processes in silicon nitride: these will be obtained from a combination of studies of electrical conductivity, galvanic cell emf and mass diffusion. Single crystals would be ideal for such studies but the author is not aware of any serious

attempts to provide them. In the absence of single crystals, well characterized CVD Si_3N_4 would be the next preferred material.

(2) Nitridation studies on specially prepared high-purity powder, and single crystal silicon material, should be continued with the object of improving understanding of the effects of commonly occurring metallic impurities, and also of the role of gaseous contaminants (O_2 , H_2O) in the N_2 and, particularly of the mechanism whereby H_2 affects the reaction so markedly. Strong emphasis should be placed on microscopy.

(3) Although extensive electrical property data exist for "thin" film silicon nitride, there is little relating to bulk material to serve as a firm basis for comparison with those for nitride ceramics in general.

For such studies, single crystals would be ideal but, as none is yet available, measurements on CVD material and high purity RBSN would be worth making. Research in this area could be justified in its own right and useful properties might emerge if impurity effects are understood and controlled.

(4) Little is known of the processes controlling high-temperature corrosion and, in particular, of the effects of impurities in the ceramic and of the composition of the corroding atmosphere. Experiments could be designed to produce data of value to the science of material degradation in general, apart from their particular relevance to the successful exploitation of RBSN in high-temperature engineering.

(5) In the many studies of room-temperature strength, sparse attention has been given to fractography. This offers the only direct means of identifying the critical defect in RBSN. Efforts should also be made to establish the nature and origins of the diffuse regions visible using polarized light microscopy.

(6) Understanding seems to be improving of the processes determining high-temperature creep behaviour. Now that high-purity RBSN can be made and control exercised over fabrication variables, studies might profitably be undertaken with the object of correlating creep behaviour with fracture face composition, using Auger analysis.

(7) Slip-casting silicon powder, which is currently exploited, could be an effective way of forming a uniform powder compact having optimum characteristics for the nitriding stage. The technology

would benefit from studies of the rheology of silicon powders, giving due regard to the silica layers covering the particles.

10.2. Fabrication technology and properties of RBSN

(1) An accepted principle of ceramics technology is that, for effective control to be exercised over microstructure, and hence properties, careful attention must be given to "starting powders". Unfortunately, this has not been generally adhered to in development, to date, of RBSN.

Concerted efforts should now be directed towards the tailoring of silicon powders to optimize their forming characteristics, the course of the nitriding process and the final microstructure. Studies should embrace availability of silicon ingot, comminution and adjustment of powder composition. Attention to the overall economics of powder preparation is essential, though the potential of the material in advanced engineering must also be borne in mind.

(2) Pressing faults and microstructural changes which occur during Ar-sintering are possible precursors to strength-limiting defects in the nitrated material and need to be controlled. Therefore, studies should embrace the "green" powder compact, before and after Ar-sintering.

(3) Studies of the nitriding of powder compacts should be extended with the object of generating data relating to transient temperature gradients arising from the reaction exotherm, and to permeability changes as the reaction proceeds. With the help of mathematical modelling it is then possible to extract the values of the relevant parameters and use them for extrapolation to the industrial scale.

These simulation/modelling procedures, which are part of the standard chemical engineering practice, offer a logical route towards designing appropriate basic experiments, and eventually optimizing industrial nitriding schedules and furnace loadings.

(4) The technologically important properties of RBSN would be improved if ways could be found to infill the porosity after fabrication. It should be possible, for example, to infiltrate liquid silicon to develop a microstructure similar to that of REFEL* silicon carbide. The author is aware that *ad hoc* attempts have been made to achieve this but, so

far, apparently, without success. The chances of success would be improved if systematic and carefully designed experiments were carried out calling upon, and if necessary generating, the necessary basic data.

Developing means to increase the density of the surface regions of RBSN should not prove too difficult, and the rewards would certainly justify the effort.

(5) The full exploitation of RBSN would be encouraged if reliable joining techniques could be developed. Studies should embrace silicon nitride/silicon nitride and silicon nitride/metal joins.

Note added in proof

In a recent paper [159] the influence of H₂ additions to N₂ on the strength, structure and composition of RBSN is discussed. This paper also brings together many of the ideas developed by Dr Lindley and his colleagues at The Admiralty Marine Technology Establishment in their commendable efforts to understand the mechanism of reaction-bonding and to optimize mechanical properties. It would seem appropriate here to summarize below the points at which their ideas differ from those developed here, and where they coincide.

(i) The AMTE group considers the SiO/N₂ reaction as the dominant one in the normal nitriding (i.e. in N₂) process; this is at variance with the arguments developed here.

(ii) The author considers that all vapour phase reactions lead to α -Si₃N₄ (or amorphous Si₃N₄); the AMTE group favours Si vapour leading to β -Si₃N₄.

(iii) The views coincide regarding the nature of the reaction (but not of the mechanisms) and reaction product when H₂ is added.

(iv) The AMTE group regard the strength-limiting defect as an intrinsic feature of the microstructure of RBSN, whereas the present author favours extrinsic, Fe-induced defects.

Acknowledgements

During the 5 years he spent working with the author at Leeds, Dr Alan Atkinson made a vital contribution to the understanding of the mechanism of the reaction between silicon and nitrogen, and his research formed a sound basis for much of our subsequent work. That part of the review

*REFEL: Self-bonded SiC manufactured by British Nuclear Fuels, Ltd, Warrington, WA3 6AS, UK.

concerned with the kinetics of the various possible nitriding reactions was based on the very comprehensive notes kindly made available by Dr Atkinson. It is a special pleasure for the author to acknowledge this help and also the lengthy discussions he has had with Dr Atkinson since his departure for Harwell.

Of the many research colleagues who have all made, in their own particular ways, real contributions to the background to the review, the author is especially grateful to Dr E. W. Roberts for his help with microstructural work and its interpretation, and particularly for his patient reading of the draft and his many constructive criticisms.

Special thanks are due to Dr Frank Riley who, through his deep involvement in, and committed enthusiasm for the silicon nitride research programme, has in so many ways made his contribution.

Throughout the research, the presentation of the Leeds work has had the able support of Mr Eric Daniels and his staff in the Photography Department, and of the secretarial staff of the Department of Ceramics. The author is very grateful to all these colleagues.

The Science Research Council has very generously supported the author's research over many years and this is gratefully acknowledged. The financial and scientific support given by the Director, Admiralty Marine Technology Establishment, is gratefully acknowledged, and the author is especially indebted to colleagues from that establishment for the many helpful and enjoyable discussions. It is a pleasure also to acknowledge the financial support received from the European Research Office.

Finally, the author is more than grateful to his wife and family for their patience.

References

1. K. H. JACK, *Trans. Brit. Ceram. Soc.* **72** (1973) 376.
2. *Idem*, *J. Mater. Sci.* **11** (1976) 1135.
3. F. L. RILEY (editor), "Nitrogen Ceramics" (Noordhoff, Leyden, 1977).
4. N. L. PARR and E. R. W. MAY, *Proc. Brit. Ceram. Soc.* **7** (1967) 81.
5. J. J. BURKE, A. E. GORUM and R. N. KATZ (editors), "Ceramics for High-Performance Applications" (Brook Hill, Chestnut Hill, Mass., 1974).
6. B. J. DALGLEISH and P. L. PRATT, *Proc. Brit. Ceram. Soc.* **25** (1975) 295.
7. D. G. S. DAVIES, *ibid.* **22** (1973) 429.
8. P. E. D. MORGAN, "Nitrogen Ceramics", edited by F. L. Riley (Noordhoff, Leyden, 1977) p. 23.
9. L. PAULING, "The Nature of the Chemical Bond", 3rd edn. (Cornell University Press, Ithaca, N.Y., 1960) p. 98.
10. O. GLEMSER, N. BELETZ and P. NAUMANN, *Z. Anorg. Chem.* **291** (1957) 51.
11. E. T. TURKDOGAN, P. M. BILLS and V. A. TIPPETT, *J. Appl. Chem.* **8** (1958) 296.
12. W. D. FORGENG and B. F. DECKER, *Trans. AIME* **212** (1958) 343.
13. S. N. RUDDLESDEN and P. POPPER, *Acta. Cryst.* **11** (1958) 465.
14. D. S. THOMPSON and P. L. PRATT, "Science of Ceramics", Vol. 3, edited by G. H. Stewart (Academic Press, London, 1967) p. 33.
15. P. GRIEVESON, K. H. JACK and S. WILD, "Special Ceramics 4", edited by P. Popper (British Ceramic Research Association, Stoke-on-Trent, 1968) p. 237.
16. S. WILD, P. GRIEVESON and K. H. JACK, "Special Ceramics 5", edited by P. Popper (British Ceramic Research Association, Stoke-on-Trent, 1972) p. 385.
17. I. COLQUHOUN, S. WILD, P. GRIEVESON and K. H. JACK, *Proc. Brit. Ceram. Soc.* **22** (1973) 207.
18. H. F. PRIEST, F. C. BURNS, G. L. PRIEST and E. C. SKAAR, *J. Amer. Ceram. Soc.* **56** (1973) 395.
19. A. J. EDWARDS, D. P. ELIAS, M. W. LINDLEY, A. ATKINSON and A. J. MOULSON, *J. Mater. Sci.* **9** (1974) 516.
20. K. KIJIMA, K. KATO, Z. INOUE and H. TANAKA, *ibid.* **10** (1975) 362.
21. K. NIIHARA and T. HIRAI, *ibid.* **11** (1976) 593.
22. R. MARCHAND, Y. LAURENT and J. LANG, *Acta Cryst.* **B25** (1969) 2157.
23. I. KOHATSU and J. W. McCAULEY, *Mater. Res. Bull.* **9** (1974) 917.
24. K. KATO, Z. INOUE, K. KIJIMA, I. KAWADA, H. TANAKA and T. YAMANE, *J. Amer. Ceram. Soc.* **58** (1975) 90.
25. C. M. B. HENDERSON and D. TAYLOR, *Trans. Brit. Ceram. Soc.* **74** (1975) 49.
26. K. NIIHARA and T. HIRAI, *J. Mater. Sci.* **12** (1977) 1233.
27. R. D. PEHLKE and J. F. ELLIOTT, *Trans. Met. Soc. AIME* **215** (1959) 781.
28. M. OLETTE, *Compt. Rend. Acad. Sci. Paris* **244** (1957) 1033.
29. P. GRIEVESON and C. B. ALCOCK, "Special Ceramics", edited by P. Popper (Heywood, London, 1960) p. 183.
30. W. B. HINCKE and L. R. BRANTLEY, *J. Amer. Chem. Soc.* **52** (1930) 48.
31. JANAF Thermochemical Tables, 2nd edn. (National Bureau of Standards, Washington, 1971).
32. K. BLEGEN, "Special Ceramics 6", edited by P. Popper (British Ceramic Research Association, Stoke-on-Trent, 1975) p. 223.
33. A. HENDRY, "Nitrogen Ceramics", edited by F. L. Riley (Noordhoff, Leyden, 1977) p. 183.
34. T. G. CHART, *High Temp.-High Press.* **2** (1970) 461.

35. R. W. DAVIDGE, A. G. EVANS, D. GILLING and P. R. WILYMAN, "Special Ceramics 5", edited by P. Popper (British Ceramic Research Association, Stoke-on-Trent, 1972) p. 329.
36. J. W. HINZE and H. C. GRAHAM, *J. Electrochem. Soc.* **123** (1976) 1066.
37. M. I. MAYER and F. L. RILEY, *J. Mater. Sci.* **13** (1978) 1319.
38. *Idem*, *Proc. Brit. Ceram. Soc.* **26** (1977) 251.
39. P. KOFSTAD, "High Temperature Oxidation of Metals" (Wiley, New York, 1966).
40. B. J. WEUNSCH and T. VASILOS, Final Report 1 January 1973 to 31 March 1975. Contract No. N00014-73-C-0212 NR 032-537/8-18-72 (471) (Office of Naval Research, Washington D. C., 1975).
41. K. KIJIMA and S. SHIRASAKI, *J. Chem. Phys.* **65** (1976) 2668.
42. A. ATKINSON, A. J. MOULSON and E. W. ROBERTS, *J. Amer. Ceram. Soc.* **59** (1976) 285.
43. R. J. BROOK, "Nitrogen Ceramics", edited by F. L. Riley (Noordhoff, Leyden, 1977) p. 187.
44. P. POPPER and S. N. RUDDLESSEN, *Trans. Brit. Ceram. Soc.* **60** (1961) 603.
45. B. J. DALGLEISH and P. L. PRATT, *Proc. Brit. Ceram. Soc.* **22** (1973) 323.
46. D. R. MESSIER and P. WONG, *J. Amer. Ceram. Soc.* **56** (1973) 480.
47. A. G. EVANS and R. W. DAVIDGE, *J. Mater. Sci.* **5** (1970) 314.
48. D. FISHLOCK, *New Scientist* **29** (1966) 283.
49. A. L. CUNNINGHAM and L. G. DAVIES, SAMPE Symposium "Materials and Processes for the Seventies", Los Angeles, USA (1969).
50. C. C. EVANS, Brit. Patent 1 121 293 (1968).
51. A. ATKINSON and A. J. MOULSON, Progress Report No. 3 (1973) SRC Research Grant B/SR/7943.
52. *Idem*, Progress Report No. 4 (1974) SRC Research Grant B/SR/7943.
53. *Idem*, "Science of Ceramics 8" (British Ceramic Society, Stoke-on-Trent, 1976) p. 111.
54. A. ATKINSON, P. J. LEATT and A. J. MOULSON, *Proc. Brit. Ceram. Soc.* **22** (1973) 253.
55. A. ATKINSON and A. D. EVANS, *Trans. Brit. Ceram. Soc.* **73** (1974) 43.
56. P. LONGLAND, Ph.D. Thesis, University of Leeds (1978).
57. P. LONGLAND and A. J. MOULSON, *J. Mater. Sci.* **13** (1978) 2279.
58. R. F. HORSLEY, Ph.D. Thesis, University of Leeds (1971).
59. S. M. BOYER, D. SANG and A. J. MOULSON, "Nitrogen Ceramics", edited by F. L. Riley (Noordhoff, Leyden, 1977) p. 297.
60. A. ATKINSON and A. J. MOULSON, Progress Report No. 5 (1975) SRC Research Grant B/SR/7943.
61. C. WAGNER, *J. Appl. Phys.* **29** (1958) 1295.
62. A. G. RAVESZ, *J. Non-Crystalline Solids* **11** (1973) 309.
63. S. M. BOYER and A. J. MOULSON, *J. Mater. Sci.* **13** (1978) 1637.
64. I. LANGMUIR, *Phys. Rev. Ser. 2* **2** (1913) 329.
65. P. ARUNDALE and A. J. MOULSON, *J. Mater. Sci.* **12** (1977) 2138.
66. K. NIWANO and A. J. MOULSON, "Slip-casting of silicon powders", Report, Department of Ceramics, University of Leeds, UK (1977).
67. W. KAISER and C. D. THURMOND, *J. Appl. Phys.* **30** (1959) 427.
68. T. J. WHALEN and A. T. ANDERSON, *J. Amer. Ceram. Soc.* **58** (1975) 396.
69. J. C. SWARTZ, *ibid.* **59** (1976) 272.
70. B. METCALFE, AWRE/44/86/96, AWRE, Aldermaston, Berks. (1974).
71. N. L. PARR, R. SANDS, P. L. PRATT, E. R. W. MAY, C. R. SHAKESPEARE and D. S. THOMPSON, *Powder Met.* **8** (1961) 152.
72. H. M. JENNINGS and M. H. RICHMAN, *J. Mater. Sci.* **11** (1976) 2087.
73. L. J. BOWEN, R. J. WESTON, T. G. CARRUTHERS and R. J. BROOK, *ibid.* **13** (1978) 341.
74. D. R. MESSIER, F. L. RILEY and R. J. BROOK, *ibid.* **13** (1978) 1199.
75. W. NARUSE, M. NOJIRI and M. TADA, *J. Jap. Inst. Metals* **35** (1971) 731.
76. D. P. ELIAS and M. W. LINDLEY, *J. Mater. Sci.* **11** (1976) 1278.
77. R. B. GUTHRIE and F. L. RILEY, *ibid.* **9** (1974) 1363.
78. W. D. SCOTT, *J. Amer. Ceram. Soc.* **52** (1969) 454.
79. W. GEORGE, Ph.D. Thesis, University of Leeds (1970).
80. B. C. H. STEELE and M. A. WILLIAMS, *J. Mater. Sci.* **8** (1973) 427.
81. B. J. DALGLEISH, Ph.D. Thesis, Imperial College, London (1974).
82. W. P. CLANCY, *Microscope* **22** (1974) 279.
83. S. C. DANFORTH, H. M. JENNINGS and M. H. RICHMAN, *Metallogr.* **9** (1976) 361.
84. H. M. JENNINGS, S. C. DANFORTH and M. H. RICHMAN, *ibid.* **9** (1976) 427.
85. B. L. METCALFE, *ibid.* **11** (1978) 231.
86. J. HALLETT and B. J. MASON, *Proc. Roy. Soc.* **A247** (1958) 440.
87. R. PAMPUCH and L. STOBIERSKI, Proceedings of the 11th Conference on the Silicate Industry, Budapest (1973) p. 979.
88. V. N. GRIBKOV, V. A. SILAEV, B. V. SHCHETANOV, E. L. UMANTSEV and A. S. ISAIKIN, *Sov. Physics. Crystallogr.* **16** (1972) 852.
89. D. P. ELIAS, B. F. JONES and M. W. LINDLEY, *Powder Met. Int.* **8** (1976) 162.
90. B. F. JONES, K. C. PITMAN and M. W. LINDLEY, *J. Mater. Sci.* **12** (1977) 563.
91. A. ATKINSON, P. J. LEATT, A. J. MOULSON and E. W. ROBERTS, *ibid.* **9** (1974) 981.
92. D. CAMPOS-LORIZ and F. L. RILEY, *ibid.* **11** (1976) 195.

93. B. F. JONES and M. W. LINDLEY, *ibid.* **11** (1976) 1288.
94. S. LIN, *J. Amer. Ceram. Soc.* **58** (1975) 271.
95. J. A. MANGELS, *ibid.* **58** (1975) 354.
96. C. E. INGLIS, *Trans. Inst. Naval Architects* **55** (1913) 219.
97. A. A. GRIFFITH, *Phil. Trans. Roy. Soc. London* **A221** (1920) 163.
98. I. N. SNEDDON, *Proc. Roy. Soc.* **A187** (1946) 229.
99. G. R. IRWIN, "Handbuch der Physik", Vol. 6, edited by S. Flügge (Springer-Verlag, Berlin, 1958) p. 551.
100. F. F. LANGE, "Fracture Mechanics of Ceramics", Vol. 1, edited by R. C. Bradt, D. P. H. Hasselman and F. F. Lange (Plenum Press, New York, 1974) p. 3.
101. A. G. EVANS, *ibid.* p. 17.
102. "Fracture Toughness Testing and its Applications", ASTM Special Technical Publications No. 381 (ASTM, Philadelphia PA, 1965).
103. A. G. EVANS and T. G. LANGDON, *Prog. Mater. Sci.* **21** (1976).
104. R. W. DAVIDGE, "Mechanical Behaviour of Ceramics" (Cambridge University Press, 1978).
105. E. RYSHKEWITCH, *J. Amer. Ceram. Soc.* **36** (1953) 65 (with discussion by W. Duckworth).
106. J. W. EDDINGTON, D. J. ROWCLIFFE and J. L. HENSHALL, *Powder Met. Int.* **7** (1975) 82.
107. P. LONGLAND and A. J. MOULSON, "Nitrogen Ceramics", edited by F. L. Riley (Noordhoff, Leyden, 1977) p. 581.
108. R. W. RICE, *J. Amer. Ceram. Soc.* **59** (1976) 536.
109. *Idem*, "Treatise on Materials Science and Technology" Vol. 11, edited by R. K. MacCrone (Academic Press, New York, 1978).
110. M. E. WASHBURN and H. R. BAUMGARTNER, "Ceramics for High-Performance Applications", edited by J. J. Burke, A. E. Gorum and R. N. Katz (Brook Hill, Chestnut Hill, Mass., 1974) p. 479.
111. D. J. GODFREY and M. W. LINDLEY, *Proc. Brit. Ceram. Soc.* **22** (1973) 229.
112. D. J. GODFREY, *ibid.* **25** (1975) 325.
113. D. R. MESSIER and P. WONG, "Ceramics for High-Performance Applications", edited by J. J. Burke, A. E. Gorum and R. N. Katz (Brook Hill, Chestnut Hill, Mass., 1974) p. 181.
114. D. S. THOMPSON and P. L. PRATT, *Proc. Brit. Ceram. Soc.* **6** (1966) 37.
115. A. DINSDALE, A. J. MOULSON and W. T. WILKINSON, *Trans. Brit. Ceram. Soc.* **61** (1962) 259.
116. D. J. GODFREY, Discussion in "Nitrogen Ceramics", edited by F. L. Riley (Noordhoff, Leyden, 1977) p. 575.
117. J. T. BARNBY and R. A. TAYLOR, "Special Ceramics 5", edited by P. Popper (British Ceramic Research Association, Stoke-on-Trent, 1972) p. 311.
118. J. A. MANGELS, "Nitrogen Ceramics", edited by F. L. Riley (Noordhoff, Leyden, 1977) p. 569.
119. P. WONG and D. R. MESSIER, *Bull. Amer. Ceram. Soc.* **57** (1978) 525.
120. W. M. DAWSON, P. ARUNDALE and A. J. MOULSON, "Science of Ceramics 9" (Nederlandse Keramische Vereniging, 1977) p. 111.
121. P. ARUNDALE, Communication to British Ceramic Society Colloquium "Silicon Nitridation and Reaction Bonding", 17 May (1978).
122. A. G. EVANS and G. TAPPIN, *Proc. Brit. Ceram. Soc.* **20** (1972) 275.
123. J. A. MANGELS, "Ceramics for High-Performance Applications", edited by J. J. Burke, A. E. Gorum and R. N. Katz (Brook Hill, Chestnut Hill, Mass., 1974) p. 195.
124. G. GRATHWHOL and F. THÜMMLER, *J. Mater. Sci.* **13** (1978) 1177.
125. S. Ud. DIN and P. S. NICHOLSON, *J. Amer. Ceram. Soc.* **58** (1975) 500.
126. N. L. PARR, G. F. MARTIN and E. R. W. MAY, "Special Ceramics", edited by P. Popper (British Ceramic Research Association, Stoke-on-Trent, 1960) p. 102.
127. J. A. COPPOLA, R. C. BRADT, D. W. RICHERSON and R. A. ALLIEGRO, *Ceram. Bull.* **51** (1972) 847.
128. P. B. NOAKES and P. L. PRATT, "Special Ceramics 5", edited by P. Popper (British Ceramic Research Association, Stoke-on-Trent, 1972) p. 299.
129. B. F. JONES and M. W. LINDLEY, *J. Mater. Sci.* **10** (1975) 967.
130. L. J. COHEN and O. ISHAI, *J. Comp. Mater.* **1** (1967) 390.
131. R. B. GUTHRIE and F. L. RILEY, *Proc. Brit. Ceram. Soc.* **22** (1973) 275.
132. B. F. JONES and M. W. LINDLEY, *J. Mater. Sci.* **11** (1976) 1969.
133. J. T. MILEK, "Handbook of Electronic Materials", Vol. 3 (IFI/Plenum, New York, 1971).
134. J. J. GEBHARDT, R. A. TANZILLI and T. A. HARRIS, "Chemical Vapour Deposition", 5th International Conference, edited by J. M. Blocher, H. E. Hinterman and L. H. Hall (Electrochemical Society, New York, 1975) p. 786.
135. B. FREUDENBERG and A. J. MOULSON, University of Leeds, unpublished work.
136. J. L. KEMP and A. J. MOULSON, *Proc. Brit. Ceram. Soc.* **18** (1970) 53.
137. J. D. WALTON, *Bull. Amer. Ceram. Soc.* **53** (1974) 255.
138. W. M. WELLS, UCRL 77 95, May (1964).
139. W. B. WESTPHAL and A. SILS, MIT Laboratory for Insulation Research, April (1972) AFML-TR-72-39.
140. G. S. PERRY and T. R. MOULES, Proceedings of the 12th Symposium on Electromagnetic Windows, edited by J. N. Harris (Georgia Institute of Technology, Atlanta, GA, 1974) p. 67.
141. D. R. MESSIER and P. WONG, Proceedings of the 13th Symposium on Electromagnetic Windows, edited by H. L. Bassett and S. M. Newton (Georgia Institute of Technology, Atlanta, GA, 1976) p. 3.
142. B. TAREEV, "Physics of Dielectric Materials" (Mir, Moscow, 1975).
143. R. VON HIPPEL, "Dielectric Materials and Applications" (MIT, Cambridge, Mass., 1954).

144. J. S. THORP and R. I. SHARIF, *J. Mater. Sci.* **12** (1977) 2274.
145. G. S. PERRY, AWRE Aldermaston, Berks., UK, private communication (1977).
146. T. L. CHU, J. R. SZEDON and C. H. LEE, *J. Electrochem. Soc. Solid State Sci.* **115** (1968) 318.
147. D. J. C. YATES, *Trans. Brit. Ceram. Soc.* **54** (1955) 272.
148. A. N. SMITH, *ibid.* **54** (1955) 300.
149. J. F. COLLINS and R. W. GERBY, *J. Metals* **7** (1955) 612.
150. Data Sheet, "Nitrasil", Associated Engineering Developments Ltd, Rugby, UK.
151. Data Sheet, Advanced Materials Engineering Ltd, Gateshead, UK.
152. W. GEORGE, *Proc. Brit. Ceram. Soc.* **22** (1973) 147.
153. C. A. WERT and R. M. THOMPSON, "Physics of Solids", 2nd edn. (McGraw-Hill, New York, 1970) p. 225.
154. P. G. BARRATT and S. N. RUDDLESDEN, British Ceramic Research Association, Stoke-on-Trent, 4th Interim Report, September 1975 to February 1976 (Contract Ref. No. 16 B1.2).
155. "Handbook of Thermophysical Properties of Solid Materials", Revised edn., Vol. 1., "Elements", edited by A. Goldsmith (Macmillan, New York, 1961).
156. "Handbook of Chemistry and Physics", 54th edn., B.235 (CRC Press, Cleveland, Ohio, 1973/4).
157. J. J. NICKL and C. VON BRAUNMÜLE, *J. Less Common Metals* **37** (1974) 317.
158. A. J. MOULSON, unpublished work.
159. M. W. LINDLEY, D. P. ELIAS, B. F. JONES and K. C. PITMAN, *J. Mater. Sci.* **14** (1979) 70.

Received 31 January and accepted 9 October 1978.